



OPEN ACCESS

EDITED BY

Karansher Singh Sandhu,
Bayer Crop Science, United States

REVIEWED BY

Muhammad Norman,
Zhejiang University, China
Hafiz Muhammad Rizwan,
Fujian Agriculture and Forestry
University, China
Parviz Heidari,
Shahrood University of Technology, Iran

*CORRESPONDENCE

Muhammad Tahir ul Qamar,
tahirulqamar@gcuf.edu.pk

[†]These authors have contributed equally
to this work

SPECIALTY SECTION

This article was submitted
to Plant Genomics,
a section of the journal
Frontiers in Genetics

RECEIVED 02 September 2022

ACCEPTED 27 September 2022

PUBLISHED 11 October 2022

CITATION

Zia K, Rao MJ, Sadaqat M, Azeem F,
Fatima K, Tahir ul Qamar M,
Alshammari A and Alharbi M (2022),
Pangenome-wide analysis of cyclic
nucleotide-gated channel (CNGC) gene
family in citrus Spp. Revealed their
intraspecies diversity and potential roles
in abiotic stress tolerance.
Front. Genet. 13:1034921.
doi: 10.3389/fgene.2022.1034921

COPYRIGHT

© 2022 Zia, Rao, Sadaqat, Azeem,
Fatima, Tahir ul Qamar, Alshammari and
Alharbi. This is an open-access article
distributed under the terms of the
[Creative Commons Attribution License \(CC BY\)](#). The use, distribution or
reproduction in other forums is
permitted, provided the original
author(s) and the copyright owner(s) are
credited and that the original
publication in this journal is cited, in
accordance with accepted academic
practice. No use, distribution or
reproduction is permitted which does
not comply with these terms.

Pangenome-wide analysis of cyclic nucleotide-gated channel (CNGC) gene family in citrus *Spp.* Revealed their intraspecies diversity and potential roles in abiotic stress tolerance

Komal Zia^{1†}, Muhammad Junaid Rao^{2†}, Muhammad Sadaqat¹,
Farrukh Azeem¹, Kinza Fatima¹, Muhammad Tahir ul Qamar^{1,3*},
Abdulrahman Alshammari⁴ and Metab Alharbi⁴

¹Integrative Omics and Molecular Modeling Laboratory, Department of Bioinformatics and Biotechnology, Government College University Faisalabad (GCUF), Faisalabad, Pakistan, ²State Key Laboratory for Conservation and Utilization of Subtropical Agro-Bioresources, Guangxi Key Laboratory of Sugarcane Biology, College of Agriculture, Guangxi University, Nanning, China, ³Department of Botany and Plant Sciences, University of California Riverside (UCR), Riverside, CA, United States, ⁴Department of Pharmacology and Toxicology, College of Pharmacy, King Saud University, Riyadh, Saudi Arabia

Cyclic nucleotide-gated channels (CNGC) gene family has been found to be involved in physiological processes including signaling pathways, environmental stresses, plant growth, and development. This gene family of non-selective cation channels is known to regulate the uptake of calcium and is reported in several plant species. The pangenome-wide studies enable researchers to understand the genetic diversity comprehensively; as a comparative analysis of multiple plant species or member of a species at once helps to better understand the evolutionary relationships and diversity present among them. In the current study, pangenome-wide analysis of the CNGC gene family has been performed on five Citrus species. As a result, a total of 32 genes in *Citrus sinensis*, 27 genes in *Citrus reticulata*, 30 genes in *Citrus grandis*, 31 genes in *Atalantia buxfolia*, and 30 genes in *Poncirus trifoliata* were identified. In addition, two unique genes *CNGC13* and *CNGC14* were identified, which may have potential roles. All the identified CNGC genes were unevenly distributed on 9 chromosomes except *P. trifoliata* had genes distributed on 7 chromosomes and were classified into four major groups and two sub-groups namely I, II, III, IV-A, and IV-B. Cyclic nucleotide binding (CNB) motif, calmodulin-binding motif (CaMB), and motif for IQ-domain were conserved in Citrus *Spp.* Intron exon structures of citrus species were not exactly as same as the gene structures of *Arabidopsis*. The majority of cis-regulatory elements (CREs) were light responsive and others include growth, development, and stress-related indicating potential roles of the CNGC gene family in these functions. Both segmental and tandem duplication were involved in the expansion of the CNGC gene family in Citrus *Spp.* The miRNAs are involved in the response of CsCNGC genes towards drought stress along with having

regulatory association in the expression of these genes. Protein-Protein interaction (PPI) analysis also showed the interaction of CNGC proteins with other CNGCs which suggested their potential role in pathways regulating different biological processes. GO enrichment revealed that CNGC genes were involved in the transport of ions across membranes. Furthermore, tissue-specific expression patterns of leaves sample of *C. sinensis* were studied under drought stress. Out of 32 genes of *C. sinensis* 3 genes i.e., *CsCNGC1.4*, *CsCNGC2.1*, and *CsCNGC4.2* were highly up-regulated, and only *CsCNGC4.6* was highly down-regulated. The qRT-PCR analysis also showed that CNGC genes were highly expressed after treatment with drought stress, while gene expression was lower under controlled conditions. This work includes findings based on multiple genomes instead of one, therefore, this will provide more genomic information rather than single genome-based studies. These findings will serve as a basis for further functional insights into the CNGC gene family.

KEYWORDS

CNGC, citrus, pan-genomics, drought stress, genome-wide analysis, molecular modeling

1 Introduction

Calcium is an important macronutrient for plant growth and development and is involved in signaling pathways as a secondary messenger. It also plays a key role in the defense mechanism of plants against abiotic stress (Lecourieux et al., 2006; Kudla et al., 2018). Calcium sensor proteins belong to three main families including calmodulin (CaM) and calmodulin-like proteins (CMLs) (Yang and Poovaiah, 2003; Bender and Snedden, 2013), calcineurin-B-like proteins (CBLs) (Luan, 2009), calcium dependent protein kinases (CPKs) and calcium and calmodulin dependent protein kinase (CCaMK) (Cheng et al., 2002; Wang et al., 2015). Calcium binding to these calcium sensors induces a conformational change that triggers either a particular target protein or directly stimulates kinase activity by taking into account CPKs (Ranty et al., 2016). In contrast, several families of ion channels regulate the uptake of calcium including Cyclic nucleotide-gated channels (CNGCs), two pore channel 1 (TCP1), ionotropic glutamate receptors, and several other channels (Demidchik et al., 2018).

CNGCs belong to the nonselective cation channels that are found in both animals and plants. Plant CNGCs was first discovered in 1998 while scanning calmodulin-conjugated transporters (HvCBT1) in barley (Mäser et al., 2001). CNGCs are ligand-gated channels that are calcium permeable and involved in the interaction of cyclic nucleotides and calcium dependent signaling pathways (Talke et al., 2003). CNGCs are calcium sensors in eukaryotes while calcium is important for plant growth, development, light signaling, drought and salt stress, and pathogen tolerance (Ranty et al., 2016). CNGCs get activated by the binding of cyclic nucleotides (cNMP) and their activity gets inhibited by Ca^{2+} /CaM binding (Trudeau and Zagotta, 2002). Calcium is very helpful in regulating plant

growth under stress conditions. There are 6 TM domains (S1-S6) and a pore region in CNGCs, fifth and sixth domains along with the Cyclic nucleotide-binding domain (CNBD) and CaM binding domains are present at C-terminal. CNBD comprises a phosphate binding cassette (PBC) and a hinge region (Duszyn et al., 2019). The PBC binds to phosphate and sugar moieties of cyclic nucleotide binding (CNB) ligand and the hinge region contributes to the efficacy of ligand binding and selectivity (Li et al., 2019). CNGCs are also involved in plants responses to various abiotic and biotic stress conditions. (Jha et al., 2016).

CNGC gene family has been reported in *Arabidopsis thaliana* (Mäser et al., 2001), *Brassica oleracea* (Kakar et al., 2017), *Zea mays* (Hao and Qiao, 2018), *Ziziphus jujube Mill.* (Wang et al., 2020), *Nicotiana tabacum L.* (Nawaz et al., 2018), *Triticum aestivum L.* (Guo et al., 2018), *Oryza sativa* (Nawaz et al., 2014), *Brassica rapa* (Li et al., 2019), *Pyrus bretschneideri Rehd* (Chen et al., 2015), and *Solanum lycopersicum* (Saand et al., 2015). On the basis of the phylogenetic classification in the aforementioned plants, this gene family is classified into four major groups and the fourth group is further divided into two sub-groups namely as; I, II, III, IV-A, IV-B. A single reference genome is not enough to capture diversity present among the members of a species (Golicz et al., 2016). Thus, it brings a bias to study gene family members in plants solely based on a single genome. Therefore, it is suggested to conduct pangenome-wide analysis for gene family characterization (Tahir Ul Qamar et al., 2019). The first ever concept regarding pangenome was introduced when the pangenome of *Streptococcus agalactiae* was developed (Tettelin et al., 2005). Pangenome of a species comprises core genes that are present in all members, accessory genes that are present in few but not in all members, and unique genes that are present only in specific members (Tahir ul Qamar et al., 2020; Ismail et al., 2022; Zanini et al., 2022).

Citrus is an economically important fruit crop as it is widely used both as a fruit and as a juice (Liu et al., 2019). It is perennial crop and mostly cultivated in China, Brazil, India, United States, Mexico, Spain, and Italy (Liu et al., 2012). Citrinae is a large group of citrus fruit trees that belong to the subfamily Aurantioideae and the family Rutaceae. Based on botanical features Citrinae is categorized into three types i.e., primitive citrus, near citrus, and true citrus (Wang et al., 2017). The well-known Citrus varieties include; *Atlantia buxfolia* (Chinese box orange), *Citrus sinensis* (sweet orange), *Citrus grandis* (pummelo), *Citrus reticulata* (mandarin), *Citrus limon* (lemon), *Citrus paradisi* (grapefruit) and *Poncirus trifoliata* (Trifoliate orange) (Liu et al., 2019). Citrus varieties widely influenced by drought stress as the productivity, growth, and yield of citrus get reduced after facing drought stress (Osakabe et al., 2014). However, few drought resistant varieties are also reported which can withstand against this stress, including navel orange and trifoliate orange (Bhusal et al., 2002; Koshita and Takahara, 2004; Pingping et al., 2017).

In present study, *C. sinensis*, *C. reticulata*, *C. grandis*, *A. buxfolia*, and *P. trifoliata* were selected for pangenome-wide analysis of CNGCs gene family, as they have good quality assembled genomes and their annotations are available at chromosome level. The quality of genome assembly or sequencing directly affects the quality of results (Vaattovaara et al., 2019), therefore, the aforementioned species were preferred to reduce the biasness. CNGCs gene family has been studied in several plant species at single genome-wide level (Mäser et al., 2001; Nawaz et al., 2014, 2018; Chen et al., 2015; Saand et al., 2015; Kakar et al., 2017; Guo et al., 2018; Hao and Qiao, 2018; Li et al., 2019; Wang et al., 2020), but no pan-genome-wide analysis has been performed before. Therefore, current study aims to provide a comprehensive pangenome-wide representation of CNGCs gene family in citrus species, which will serve as the foundation for future gene family researches.

2 Materials and methods

2.1 Identification of cyclic nucleotide-gated channel family genes in *C. sinensis*, *C. reticulata*, *C. grandis*, *A. buxfolia*, and *P. trifoliata*

20 CNGC protein sequences of *A. thaliana* taken from TAIR database (<https://www.arabidopsis.org/>) (Rhee et al., 2003) were used as query and BLASTp search was performed on Citrus pangenome to breeding database (CPBD; <https://citrus.hzau.edu.cn/>) (Liu et al., 2022) against *C. sinensis* v2.0, *A. buxfolia* v2.0, *P. trifoliata* v1.0, *C. reticulata* v2.0, and *Citrus grandis* (L.) Osbeck cv. Wanbaiyou v1.0. The resulting BLAST hits were manually processed to remove duplicates and isoforms and the final hits were used for further analyses.

To check the presence of specific domains, databases including SMART (<https://smart.embl-heidelberg.de/>) (Schultz et al., 2000), CDD (<https://pfam.xfam.org/>) (Marchler-bauer et al., 2011), and HMMER (<https://www.ebi.ac.uk/Tools/hmmer/search/hmmsearch>) (Potter et al., 2018) were used. This eliminated those sequences that didn't have specific conserved domains required for CNGC protein function. Domain architecture was constructed using the HMMER database. Molecular weight (MW), Theoretical isoelectric point (PI), Instability index (II), Aliphatic index (AI), and Grand average of hydropathy (GRAVY) were determined by using the web-based tool ProtParam available at the EXPASY server (<https://web.expasy.org/protparam>) (Gasteiger et al., 2003). Subcellular localization was determined using CELLO version 2.5 (<https://cello.life.nctu.edu.tw/>) (Yu et al., 2006).

2.2 Multiple sequence alignment and phylogenetic analysis

To comprehend the phylogenetic relationships of identified CNGCs, multiple sequence alignment of identified CNGC protein sequences of *C. sinensis*, *A. buxfolia*, *C. reticulata*, *C. grandis*, *P. trifoliata* along with already reported protein sequences of *O. sativa* (Nawaz et al., 2014), *Z. jujuba* (Wang et al., 2020), *Z. mays* (Hao and Qiao, 2018), *A. thaliana* (Köhler and Neuhaus, 2000) and *P. bretschneideri* (Chen et al., 2015) was done using ClustalW program and a phylogenetic tree was constructed by using online server IQ-tree (<https://iqtree.cibiv.univie.ac.at/>) (Nguyen et al., 2015) with Maximum Likelihood (ML) method and 1,000 replicates while other parameters were set to their default values. The tree was visualized and edited using the online server iTOL (<https://itol.embl.de/>) (Letunic and Bork, 2021).

2.3 Chromosomal location, gene structure, and conserved motif analysis

The chromosomal location, start and end sites of *C. sinensis*, *A. buxfolia*, *C. reticulata*, *C. grandis*, and *P. trifoliata* were retrieved from the CPBD database and a genetic linkage was constructed by using TBtools (Chen et al., 2020). The gene and CDS sequences of *C. sinensis*, *A. buxfolia*, *C. reticulata*, *C. grandis*, and *P. trifoliata* were retrieved from the sequence fetch option at the CPBD database (<https://citrus.hzau.edu.cn/>) (Liu et al., 2022). The GSDS v2.0 (<https://gsds.gao-lab.org/>) (Hu et al., 2015) was used for the visualization of gene structures of CsCNGCs, AbuCNGCs, CreCNGCs, CgCNGCs, and PtCNGCs. Conserved motifs were identified by using MEME (Multiple EM for Motif Elicitation) suite 5.4.1 (<https://meme-suite.org/meme/db/motifs>) (Bailey et al., 2009). All parameters were set to their default values except the number of motifs that were set to 10.

2.4 Gene duplication and promoter analysis

The location of CNGC genes in *C. sinensis*, *C. reticulata*, *C. grandis*, *A. buxfolia*, and *P. trifoliata* was retrieved from the CPBD database (<https://citrus.hzau.edu.cn/>) (Liu et al., 2022). All genes possessing $\geq 70\%$ sequence identity were considered duplicated genes (Hu et al., 2021). DnaSP v6.0 (Librado and Rozas, 2009) offline tool was used to calculate the rate of Non-synonymous (Ka) and synonymous substitutions (Ks) of duplicated gene pairs. To calculate the selection pressure that assisted in the evolution of the CNGC gene family Ka/Ks ratio was used. The formula for calculating duplication time was the following: $T = Ks/2x$ (where x represents substitutions per synonymous site per year and is equal to 6.56×10^{-9} for dicots) (He et al., 2016). The cis-elements in 2000bp coding regions of CsCNGCs, CreCNGCs, CgCNGCs, AbuCNGCs, and PtCNGCs were retrieved from the Citrus pan-genome to breeding database (CPBD, <https://www.citrus.hzau.edu.cn/>) (Liu et al., 2022). While the types, numbers, and functions of these cis-elements were analyzed by using PlantCare web-based tool (<https://bioinformatics.psb.ugent.be/webtools/plantcare/html/>) (Lescot et al., 2002).

2.5 Putative miRNA target prediction, protein-protein interaction network, and gene ontology analysis of citrus *Spp.*

Plant microRNA Encyclopedia (PmiREN; <https://pmiren.com>) database was utilized to acquire mature miRNA sequences of *C. sinensis*. For putative miRNA target prediction CDS sequences of the potential target, CsCNGCs were utilized and were submitted at the psRNATarget server (<https://www.zhaolab.org/psRNATarget/home>) (Dai et al., 2018) along with the respective mature miRNA sequences of *C. sinensis* with default considerations. The regulatory association between target CsCNGCs and predicted miRNAs was visualized using Cytoscape software (Shannon et al., 1971). The interaction among members of the CNGC protein family and other proteins from the citrus plant was predicted using the STRING database (<https://string-db.org/>). 32 CsCNGC protein sequences were uploaded to the STRING database with '*Citrus sinensis*' being selected as reference species. The level of connection used was sixth and other parameters were kept by default. PPI network was visualized and edited using Cytoscape software (Shannon et al., 1971). Citrus Pan-genome2breeding database (CPBD; <http://citrus.hzau.edu.cn/>) (Liu et al., 2022) was utilized to analyze gene ontology (GO) enrichment of Citrus *Spp.* using the gene IDs of CNGC genes.

2.6 Expression profiling of *C. sinensis* under drought stress

To demonstrate the expression of *C. sinensis* under abiotic stress (drought) in leaves, RNA-seq data was downloaded from

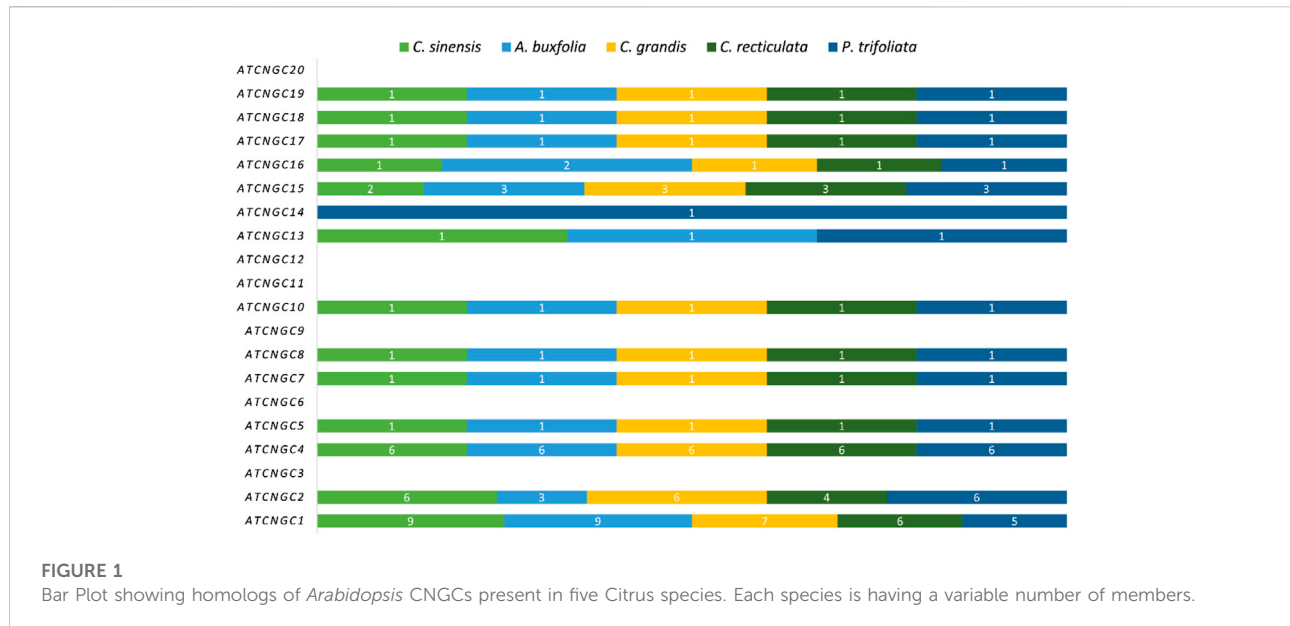
the NCBI-SRA database (<https://www.ncbi.nlm.nih.gov/sra>) (BioProject: PRJNA792482). Reference genome and GFF3 files were downloaded from the Citrus pan-genome to breeding database (CPBD, <https://citrus.hzau.edu.cn/>) (Liu et al., 2022). To check the quality of paired-end data (in FASTQ format) FASTQC was utilized and Trimmomatic was used for trimming and improving the quality of reads. Then HISAT2 was used for the alignment of reads to the *C. sinensis* v2.0 genome. To normalize gene expression in terms of Fragments per kilobase of transcripts per million mapped reads (FPKM) Cufflinks were used. The heatmap was constructed using pheatmap function of R-language (Ihaka and Gentleman, 1996).

2.7 Drought stress treatment, ribonucleic acid isolation, and quantitative real-time reverse transcription–polymerase chain

Citrus plants were grown under controlled environmental conditions in a growth chamber (having $60 \pm 3\%$ humidity, $27 \pm 2^\circ\text{C}$ temperature, and 5000 LUX light intensity) with recommended fertilizer and water treatment. Four months old citrus plants were subjected to drought stress and leaves were collected and 0, 10, and 20 days of drought stress. Control and drought-stressed leaves were harvested for RNA extraction. Zomanbio (Cat no. ZP401-2) total RNA-pure reagent (Lot#200F12F) was used to extract total RNA and the complementary DNA (cDNA) was synthesized by using Zomanbio (M-MLV, ZR102-3) reverse transcriptase kit (Beijing, ZOMAN Biotechnology Co., Ltd.) according to the manufacturer instructions. For quantitative real-time polymerase chain reaction (qRT-PCR) ChamQ universal master mix SYBR (Vazyme, Q711-02) and LongGene (Model: q2000b) fluorescence quantitative PCR instrument (Langji Scientific instrument Co., Ltd.; Hangzhou, China) were used whereas citrus actin gene was used as an internal reference. $2^{-(\Delta\Delta Ct)}$ method was applied to analyze the qRT-PCR expression data in Excel (Microsoft Corp., Redmond, WA, United States). Statistix 8.1 (Tallahassee Florida, United States) statistical software was used for analyzing all qRT-PCR data and the Excel program was used for graphs. The qPCR primer information is characterized (Supplementary Table S1).

2.8 3D Structure prediction of cyclic nucleotide-gated channels in citrus spp.

Three-dimensional (3D) structures of 13 CNGC proteins were predicted, including 9 proteins from *C. sinensis*, one from *A. buxfolia*, and two from *P. trifoliata*. Among these 13 proteins, 3D structures of 12 CNGC proteins were predicted by using AlphaFold2 (<https://colab.research.google.com/github/sokrypton/ColabFold/blob/main/AlphaFold2.ipynb>) (Jumper



et al., 2021) Whereas, the 3D structure of CsCNGC1.4 was predicted by using trRosetta (<https://yanglab.nankai.edu.cn/trRosetta/>) (Du et al., 2021) due to its length i.e., 1427aa. Protein structures were visualized by using Pymol (Yuan et al., 2017). For validation of these predicted structures SAVES server (<https://saves.mbi.ucla.edu>) was used.

3 Results

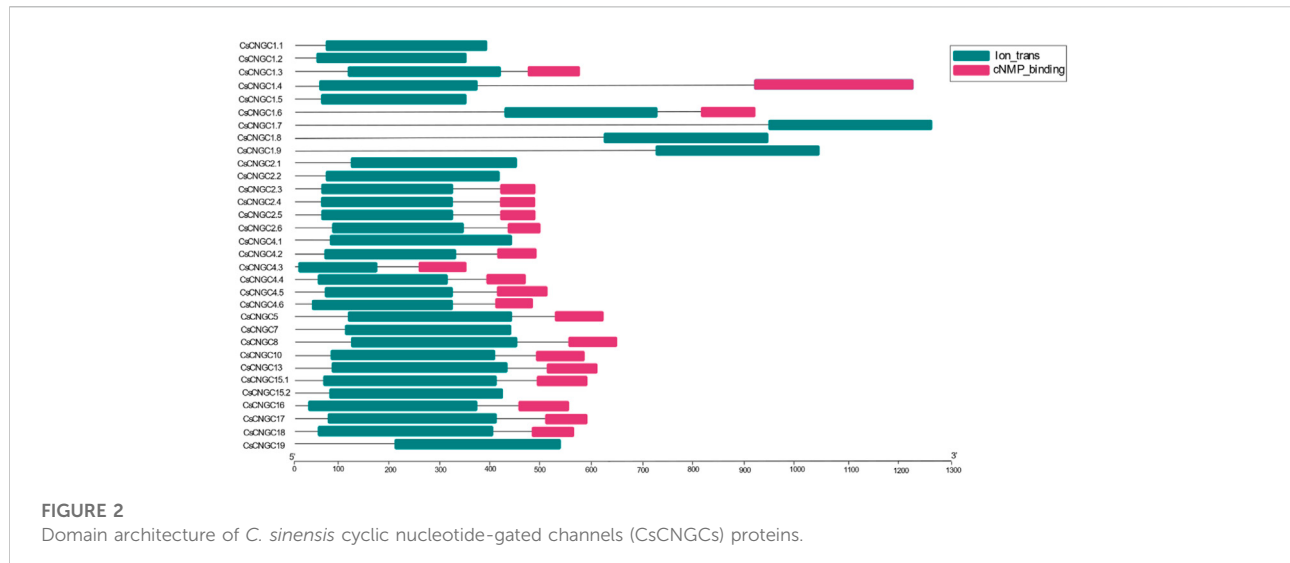
3.1 Identification of cyclic nucleotide-gated channel genes in *C. sinensis*, *C. reticulata*, *C. grandis*, *A. buxfolia*, and *P. trifoliata*

A total of 32 putative genes in *C. sinensis*, 27 genes in *C. reticulata*, 30 genes in *C. grandis*, 31 genes in *A. buxfolia*, and 30 in *P. trifoliata* were identified. The identified CNGC genes were named based on their phylogenetic relationships with CNGCs in *Arabidopsis*. Figure 1 is showing the homologs of *Arabidopsis* CNGC genes present in five species under study. Most of the identified members of *Arabidopsis* CNGCs are present in five species under study except for *AtCNGC3*, *AtCNGC6*, *AtCNGC9*, *AtCNGC11*, *AtCNGC12*, and *AtCNGC20*. All other members have a variable number of homologs present in five Citrus species. Further, two unique genes were identified: *CNGC13* and *CNGC14*. *CNGC13* is present in three plant species including *C. sinensis*, *A. buxfolia*, and *P. trifoliata* while absent in *C. grandis* and *C. reticulata*. *CNGC14* is present in only one plant species, *P. trifoliata* while being absent in the other four species.

Conserved domains that were predicted in *C. sinensis*, *A. buxfolia*, *C. reticulata*, *C. grandis*, and *P. trifoliata* include Cyclic Nucleotide Binding Domain (CNBD or cNMP), Ion trans (IT), Cap family effector domain (CAP_ED) and other ion trans domains (Supplementary Table S2). Ion trans and cNMP binding domains were the most conserved among all. Domain architecture was constructed according to the prediction results of the HMMER database. cNMP binding domain was not present in *CsCNGC1.1*, *CsCNGC1.2*, *CsCNGC1.5*, *CsCNGC1.7*, *CsCNGC1.8*, *CsCNGC1.9*, *CsCNGC2.1*, *CsCNGC2.2*, *CsCNGC4.1*, *CsCNGC7*, *CsCNGC15.2* and *CsCNGC19* according to prediction results of HMMER database but SMART database prediction confirms the presence of cNMP binding domain in these proteins. The domain architecture of *C. sinensis* is given in (Figure 2).

Ion trans domain was absent in *CreCNGC1.2*, and *CreCNGC1.6* according to HMMER database prediction. While CDD prediction confirms the presence of the Ion trans domain in *CreCNGC1.6*. Results of the HMMER database demonstrate the absence of the cNMP binding domain in *CreCNGC1.1*, *CreCNGC1.3*, *CreCNGC1.4*, *CreCNGC2.1*, *CreCNGC4.1*, *CreCNGC7*, *CreCNGC15.1*, *CreCNGC15.3*, and *CreCNGC19* according to prediction. Domains predicted by the SMART database indicated the presence of the cNMP binding domain in these proteins (Supplementary Figure S1).

The following proteins of *C. grandis* *CgCNGC1.1*, *CgCNGC1.2*, *CgCNGC1.3*, *CgCNGC1.4*, *CgCNGC1.5*, *CgCNGC1.6*, *CgCNGC2.1*, *CgCNGC2.2*, *CgCNGC4.1*, *CgCNGC7*, *CgCNGC15.1*, *CgCNGC15.3*, and *CgCNGC19* didn't have cNMP binding domain as per HMMER database prediction. Whereas, the cNMP binding domain was predicted to be present in all these proteins

**FIGURE 2**

Domain architecture of *C. sinensis* cyclic nucleotide-gated channels (CsCNGCs) proteins.

except CgCNGC1.3 as supported by SMART prediction (Supplementary Figure S2).

AbuCNGC1.1, AbuCNGC1.3, AbuCNGC1.5, AbuCNGC1.7, AbuCNGC1.8, AbuCNGC1.9, AbuCNGC2.1, AbuCNGC4.1, AbuCNGC7, AbuCNGC15.1, AbuCNGC15.3, and AbuCNGC19 are those aforementioned proteins of *A. buxfolia* that have cNMP binding domain absent in them according to the prediction of HMMER database. But taking into account the domains predicted in these proteins by the SMART database the cNMP binding domain was present in all of them. Prediction results of the HMMER, SMART, and CDD database demonstrate the absence of the Ion trans domain in AbuCNGC1.4 (Supplementary Figure S3).

PtCNGC proteins that have cNMP binding domain absent in them include PtCNGC1.1, PtCNGC1.3, PtCNGC1.4, PtCNGC1.5, PtCNGC2.1, PtCNGC2.2, PtCNGC2.3, PtCNGC2.4, PtCNGC4.1, PtCNGC7, PtCNGC14, PtCNGC15.1, PtCNGC15.3 and PtCNGC19 as predicted by HMMER database. But the cNMP binding domain was absent only in PtCNGC14 and present in all the other aforementioned PtCNGCs (Supplementary Figure S4). Details of CNGCs reported in other plants are shown in Table 1.

3.2 Physiochemical properties and subcellular localization analysis of cyclic nucleotide-gated channels in citrus *Spp.*

The detailed physio-chemical properties of 150 CNGC proteins of five Citrus *Spp.* are shown in (Table 2). *C. sinensis* had protein length ranging from 492–1553aa, molecular weight (MW) ranging from 56.13–177.77 (kDa), and Isoelectric point (PI) ranging

from 6.38–9.52, Instability index (II) was above 40 for 25 proteins of *C. sinensis*, indicating that most of the proteins were unstable. GRAVY values of 29 proteins of *C. sinensis* were negative indicating that the majority of proteins were hydrophilic. Results of subcellular localization suggested that all putative CsCNGC proteins were present in the plasma membrane.

The protein length of CreCNGCs ranged from 371–1513aa, molecular weight (MW) ranged from 43.15–173.29 (kDa), Isoelectric point (PI) ranged from 6.33–9.44, 21 CreCNGCs proteins were unstable as they have II above 40. GRAVY values of 24 CreCNGCs were negative indicating that maximum proteins were hydrophilic. Only CreCNGC1.3 was localized in the plasma membrane and nuclear compartments while the rest were found to be localized in the plasma membrane.

CgCNGCs have protein lengths ranging from 299–1289aa, molecular weight (MW) ranging from 34.21–147.32 (kDa), Isoelectric point (PI) ranging from 6.06–9.52, Most of the proteins (22) of *C. grandis* were unstable as these proteins have II greater than 40. GRAVY values for 27 proteins of *C. grandis* were negative suggesting that these proteins were hydrophilic. All of the CgCNGCs were found to be localized in the plasma membrane.

A. buxfolia had protein length ranging from 286–1335aa, molecular weight (MW) ranging from 33.62–766.01 (kDa), Isoelectric point (PI) ranging from 6.02–9.7, Instability index (II) was above 40 for 21 proteins of *A. buxfolia* revealing that most of the proteins were unstable in the test tube. 24 proteins of *A. buxfolia* were hydrophilic as their GRAVY values were negative while 7 proteins were hydrophobic as their GRAVY values were positive. Results of subcellular localization demonstrated that all AbuCNGC proteins were found to be present in the plasma membrane.

TABLE 1 Summary of CNGCs reported in other plants.

Plant name	Cotyledon	Group I	Group II	Group III	Group IV-A	Group IV-B	Total	References
<i>Arabidopsis thaliana</i>	Dicot	6	5	5	2	2	20	Mäser et al. (2001)
<i>Brassica rapa</i>	Dicot	7	5	6	9	3	30	Li et al. (2019)
<i>Brassica oleracea</i>	Dicot	3	5	6	3	9	26	Kakar et al. (2017)
<i>Zea mays</i>	monocot	3	2	3	1	3	12	Hao and Qiao, (2018)
<i>Pyrus bretschneideri Rehd.</i>	Dicot	7	2	5	2	5	21	Chen et al. (2015)
<i>Oryza sativa</i>	monocot	3	3	5	2	3	16	Nawaz et al. (2014)
<i>Ziziphus jujuba Mill.</i>	Dicot	3	2	6	1	3	15	Wang et al. (2020)
<i>Triticum aestivum L.</i>	monocot	4	12	19	4	8	47	Guo et al. (2018)
<i>Nicotiana tabacum L.</i>	Dicot	7	6	12	3	7	35	Nawaz et al. (2018)
<i>Solanum lycopersicum L.</i>	Dicot	6	3	5	1	3	18	Saand et al. (2015)

P. trifoliata's protein length ranged from 575–1250aa, molecular weight (MW) ranged from 12.10–143.55 (kDa) for *P. trifoliata*, Isoelectric point (PI) ranged from 6.62–9.54, Instability index (II) was above 40 for 25 proteins of *P. trifoliata* suggesting that most proteins were unstable. 25 PtCNGC proteins were hydrophilic because GRAVY values for these proteins were negative. For *P. trifoliata* PtCNGC2.5 was localized in the plasma membrane as well as cytoplasmic and nuclear compartments while the rest were localized in the Plasma membrane. Hence, we can conclude that most of the proteins of Citrus Spp. were basic, unstable, hydrophilic, and localized in the Plasma membrane. The Citrus CNGC proteins that were stable can be used as a biomarker for further studies.

3.3 Phylogenetic analysis

In total, 20 AtCNGCs, 16 OsCNGCs, 12 ZmCNGCs, 21 PbrCNGCs, 15 ZjCNGCs, 32 CsCNGCs, 27 CreCNGCs, 30 CgCNGCs, 31 AbuCNGCs, and 30 PtCNGCs genes were classified into four groups and the fourth group was further classified into two sub-groups, I, II, III, IV-A, IV-B each containing the different number of members. The maximum number of members were present in Group IV (84 members) divided into the clade of Group IV-B with 71 members: two members from *A. thaliana* (AtCNGC2 and 4), three from *O. sativa* (OsCNGC2, 4a and 4b), three from *Z. mays* (ZmCNGC10,11 and 12), five from *P. bretschneideri* (PbrCNGC2, 4, 7, 8 and 9) three from *Z. jujuba* (ZjCNGC13, 14 and 15), 12 from *C. sinensis* (CsCNGC4.1-4.6 and CsCNGC2.1-2.6), 10 from *C. reticulata* (CreCNGC4.1-4.6 and CreCNGC2.1-2.4), 12 from *C. grandis* (CgCNGC4.1-4.6 and CgCNGC2.1-2.6), 9 from *A. buxfolia* (AbuCNGC4.1-4.6, AbuCNGC2.1-2.3) and 12 from *P. trifoliata* (PtCNGC4.1-4.6 and PtCNGC2.1-2.6) and Group IV-A with 13 members: two from *A. thaliana* (AtCNGC19 and 20), two from *O. sativa* (OsCNGC19a and 19b), one from *Z.*

mays (ZmCNGC9), two from *P. bretschneideri* (PbrCNGC19 and 20), one from *Z. jujuba* (ZjCNGC12), one from *C. sinensis* (CsCNGC19), one from *C. reticulata* (CreCNGC19), one from *C. grandis* (CgCNGC19), one from *A. buxfolia* (AbuCNGC19) and one from *P. trifoliata* (PtCNGC19). The minimum number of members present in the clade of group II with 29 members two from *Z. mays* (ZmCNGC4 and ZmCNGC5), three from *O. sativa* (OsCNGC5a, OsCNGC5b, and OsCNGC5c), two from *Z. jujube* (ZjCNGC4 and ZjCNGC5), two from *P. bretschneideri* (PbrCNGC5 and PbrCNGC6), five from *A. thaliana* (AtCNGC5, AtCNGC6, AtCNGC7, AtCNGC8, and AtCNGC9), three from *C. sinensis* (CsCNGC5, CsCNGC7, and CsCNGC8), three from *C. reticulata* (CreCNGC5, CreCNGC7, and CreCNGC8), three from *C. grandis* (CgCNGC5, CgCNGC7, and CgCNGC8), three from *A. buxfolia* (AbuCNGC5, AbuCNGC7, and AbuCNGC8), three from *P. trifoliata* (PtCNGC5, PtCNGC7, and PtCNGC8). The number of members in other groups was also different as Group I had 66 members and Group III had 56 members in total (Figure 3).

CNGCs from every group shared a clade with *Arabidopsis* CNGC members that are a dicot, which demonstrates that CNGCs emerged after the divergence of monocots and dicots. The close association of CNGC members in Citrus Spp. with AtCNGCs demonstrates that these are orthologs of CNGCs in *Arabidopsis*. Members of the same group might have similar structures and functions. The results of phylogenetic analysis of CNGCs in Citrus Spp. were different than those in *A. thaliana*, *O. sativa*, *T. aestivum*, *N. tabacum*, *B. oleracea*, *B. rapa*, *P. bretschneideri*, *Z. jujuba* as current analysis revealed that Group IV clade was largest with 84 members in total and the clade of group II was smallest with 29 members. The number of members in group IV was almost consistent with the previously reported number of members in *Z. mays*, which had 86 members in group IV. The minimum number of members present in the clade of group I was 25. Overall, the number of members was different in each

TABLE 2 Physiochemical properties of Citrus Spp.

Gene Name	Protein id	Group	TM domains	Chr	Start	End	Strand	Protein length (AA)	Molecular weight (MW)	Isoelectric point (PI)	Instability index (II)	Aliphatic index (AI)	Grand average of hydrophathy (GRAVY)	Subcellular localization
<i>C. sinensis</i> CNGCs														
CsCNGC1.1	Cs9g_pb020800.1	I	6	9	24,382,883	24,387,758	+	927	106,182.81	9.47	49.27-unst	92.39	-0.115	Plasma membrane
CsCNGC1.2	Cs9g_pb020720.2	I	5	9	24,280,566	24,287,342	+	649	74,468.57	9.07	41.33-unst	90.59	-0.044	Plasma membrane
CsCNGC1.3	Cs2g_pb014570.1	I	5	2	12,798,466	12,807,926	-	668	77,016.05	9.23	50.97-unst	92.67	-0.052	Plasma membrane
CsCNGC1.4	Cs9g_pb020710.1	I	11	9	24,272,155	24,279,547	-	1,427	164,185.99	9.01	48.08-unst	89.68	-0.222	Plasma membrane
CsCNGC1.5	Cs9g_pb020550.1	I	4	9	24,081,889	24,084,603	-	572	65,811.13	8.57	40.46-unst	98.42	-0.016	Plasma membrane
CsCNGC1.6	Cs9g_pb020690.1	I	6	9	24,259,820	24,265,542	-	958	109,207.77	8.47	43.41-unst	89.23	-0.18	Plasma membrane
CsCNGC1.7	Cs9g_pb020610.1	I	12	9	24,129,588	24,139,417	-	1,553	177,772.54	8.3	42.08-unst	95.86	-0.04	Plasma membrane
CsCNGC1.8	Cs9g_pb020780.1	I	12	9	24,345,495	24,353,666	+	1,181	136,124.69	8.62	43.7-unst	93.65	0.018	Plasma membrane
CsCNGC1.9	Cs9g_pb020790.1	I	11	9	24,357,999	24,370,147	+	1,290	147,302.3	8.7	40.01-unst	101.17	0.09	Plasma membrane
CsCNGC2.1	Cs6g_pb020330.1	IV-B	7	6	21,816,537	21,821,804	+	714	81,992.71	9.51	48.62-unst	93.24	-0.024	Plasma membrane
CsCNGC2.2	Cs6g_pb020320.1	IV-B	6	6	21,803,582	21,807,522	-	668	76,724.79	9.44	51.02-unst	100.24	0.04	Plasma membrane
CsCNGC2.3	Cs9g_pb014190.4	IV-B	5	9	17,045,621	17,063,515	+	839	95,658.31	6.72	38.76	97.02	-0.081	Plasma membrane
CsCNGC2.4	Cs3g_pb003680.1	IV-B	5	3	9,615,973	9,627,834	+	817	93,479.69	6.62	35.54	97	-0.111	Plasma membrane
CsCNGC2.5	Cs8g_pb010740.1	IV-B	5	8	11,455,619	11,467,550	-	817	93,333.42	6.72	35.97	96.04	-0.131	Plasma membrane
CsCNGC2.6	Cs1g_pb001090.1	IV-B	5	1	3,825,286	3,830,902	-	822	94,303.4	6.42	39.7	96.55	-0.18	Plasma membrane
CsCNGC4.1	CsUn_pb001730.1	IV-B	7	un	2,087,324	2,092,767	-	696	80,863.76	8.8	55.85-unst	88.92	-0.174	Plasma membrane
CsCNGC4.2	Cs3g_pb003330.1	IV-B	5	3	5,449,938	5,460,243	-	834	95,075.26	7.35	34	99.74	-0.08	Plasma membrane
CsCNGC4.3	Cs4g_pb023890.1	IV-B	3	4	24,723,554	24,729,965	+	492	56,135.04	7.33	36.1	100.45	-0.08	Plasma membrane
CsCNGC4.4	Cs2g_pb007660.1	IV-B	6	2	2,423,659	2,427,730	-	785	89,767.74	6.38	45.13-unst	89.66	-0.202	Plasma membrane
CsCNGC4.5	Cs4g_pb023340.1	IV-B	5	4	25,225,304	25,229,876	-	888	99,688.53	7.64	44.69-unst	97.72	-0.133	Plasma membrane
CsCNGC4.6	Cs4g_pb019870.1	IV-B	5	4	21,495,102	21,501,116	-	884	99,608.21	6.68	38.99	96.47	-0.135	Plasma membrane
CsCNGC5	Cs4g_pb000740.1	II	5	4	952,948	960,923	-	734	84,009.72	9.04	49.85-unst	87.56	-0.171	Plasma membrane
CsCNGC7	Cs1g_pb010020.2	II	5	1	15,065,043	15,071,550	+	747	85,912.18	9.25	46.4-unst	93.82	-0.137	Plasma membrane
CsCNGC8	Cs1g_pb01030.1	II	5	1	15,075,187	15,080,475	+	749	86,209.43	9.22	50.26-unst	86.28	-0.189	Plasma membrane
CsCNGC10	Cs9g_pb020770.1	I	5	9	24,338,616	24,343,695	+	710	81,613.47	9.14	46.55-unst	88.84	-0.136	Plasma membrane
CsCNGC13	Cs5g_pb002630.1	I	5	5	1,720,153	1,724,660	+	723	83,314.54	9.17	51.42-unst	88.2	-0.184	Plasma membrane
CsCNGC15.1	Cs8g_pb020390.1	III	5	8	20,533,061	20,537,081	+	698	80,196.86	9.3	52.12-unst	92.18	-0.147	Plasma membrane
CsCNGC15.2	Cs6g_pb003650.1	III	6	6	7,204,408	7,208,020	+	711	81,667.77	9.3	52.11-unst	91.04	-0.102	Plasma membrane
CsCNGC16	Cs5g_pb011010.1	III	6	5	5,013,563	5,016,560	+	691	79,200.38	8.1	51.35-unst	95.55	-0.043	Plasma membrane
CsCNGC17	Cs4g_pb001750.1	III	5	4	1,625,519	1,631,583	+	723	83,201.18	9.38	40.68-unst	91.43	-0.187	Plasma membrane
CsCNGC18	Cs2g_pb028120.1	III	7	2	3,1,331,822	31,335,320	-	732	83,366.68	8.38	44.03-unst	91.53	-0.053	Plasma membrane
CsCNGC19	Cs5g_pb020580.2	IV-A	6	5	22,133,938	22,155,313	-	775	89,042.58	9.52	45.27-unst	86.69	-0.222	Plasma membrane
<i>C. reticulata</i> CNGCs														
CreCNGC1.1	Cre9g_024,150.1	I	5	9	30,685,880	30,690,506	-	961	109,420.49	9.44	48.06-unst	93.09	-0.101	Plasma membrane
CreCNGC1.2	Cre2g_019,820.1	I	1	2	16,922,647	16,925,029	-	371	43,157.28	8.42	55.6-unst	81.19	-0.359	Plasma membrane

(Continued on following page)

TABLE 2 (Continued) Physiochemical properties of *Citrus Spp.*

Gene Name	Protein id	Group	TM domains	Chr	Start	End	Strand	Protein length (AA)	Molecular weight (MW)	Isoelectric point (PI)	Instability index (II)	Aliphatic index (AI)	Grand average of hydrophathy (GRAVY)	Subcellular localization
CreCNGC1.3	Cre9g_024,250.1	I	5	9	30,796,869	3,0801,729	+	958	109,413.81	8.96	48.74-unst	85.85	-0.339	Plasma membrane, Nuclear
	Cre9g_024,430.1	I	4	9	30,990,029	30,992,744	+	572	65,837.21	8.57	40.31-unst	99.11	-0.006	Plasma membrane
CreCNGC1.4	Cre9g_024,260.1	I	6	9	30,808,308	30,814,126	+	962	109,643.04	8.62	41.49-unst	87.34	87.34	Plasma membrane
	Cre9g_024,380.1	I	12	9	30,935,435	30,944,980	+	1,513	173,290.51	8.49	42.46-unst	96.34	-0.029	Plasma membrane
CreCNGC1.6	Cre6g_023,700.1	IV-B	6	6	25,763,432	25,767,287	-	671	77,122.25	9.38	51.84-unst	99.21	0.037	Plasma membrane
	Cre9g_017,070.1	IV-B	3	9	23,979,122	23,990,027	+	583	66,299.41	6.52	35.75	99.64	-0.094	Plasma membrane
CreCNGC2.2	Cre9g_014,190.1	IV-B	5	9	16,533,233	16,544,587	-	816	93,352.54	6.9	33.85	96.39	-0.126	Plasma membrane
	Cre1g_003,650.1	IV-B	5	1	3,866,987	3,872,463	-	822	94,327.41	6.33	39.86	97.03	-0.181	Plasma membrane
CreCNGC2.4	Cre4g_013,910.1	IV-B	7	4	19,140,542	19,146,068	+	696	80,893.79	8.8	55.85-unst	88.78	-0.178	Plasma membrane
	Cre3g_025,930.2	IV-B	7	3	29,055,761	29,066,087	+	869	99,262.3	7.14	33.61	100.99	-0.04	Plasma membrane
CreCNGC4.3	Cre4g_003,630.1	IV-B	6	4	2,657,893	2,664,366	-	633	72,434.98	8.78	36.21	101.49	0.002	Plasma membrane
	Cre2g_002,210.1	IV-B	5	2	1,245,194	1,249,035	-	785	89,717.54	6.53	44.43-unst	88.79	-0.226	Plasma membrane
CreCNGC4.4	Cre4g_002,970.1	IV-B	5	4	2,152,171	2,156,534	+	888	99,743.65	7.92	44.94-unst	97.84	-0.137	Plasma membrane
	Cre4g_006,610.1	IV-B	5	4	5,039,735	5,045,661	+	884	99,723.29	6.79	39.14	96.02	-0.143	Plasma membrane
CreCNGC4.6	Cre4g_026,070.1	II	5	4	28,785,823	28,793,750	+	735	84,068.75	9.04	50.16-unst	87.18	-0.175	Plasma membrane
	Cre1g_009,420.1	II	5	1	14,655,919	14,661,193	+	747	85,925.18	9.25	45.18-unst	93.43	-0.143	Plasma membrane
CreCNGC8	Cre1g_009,430.1	II	2	1	14,666,579	14,670,161	+	534	61,818.9	8.86	50.19-unst	82.87	-0.298	Plasma membrane
	Cre9g_024,180.1	I	5	9	30,730,436	30,735,418	-	710	81,613.47	9.14	46.55-unst	88.84	-0.136	Plasma membrane
CreCNGC10	Cre8g_016,390.1	III	7	8	1,5741,807	15,745,297	-	729	83,420.51	9.13	49.51-unst	92.25	-0.121	Plasma membrane
	Cre8g_016,380.1	III	5	8	15,732,273	15,735,541	-	698	80,196.86	9.3	52.12-unst	92.18	-0.147	Plasma membrane
CreCNGC15.2	Cre6g_004,960.1	III	6	6	10,274,134	10,277,745	+	711	81,722.85	9.33	52.22-unst	91.04	-0.108	Plasma membrane
	Cre5g_004,550.1	III	4	5	3,074,499	3,077,145	+	604	69,195.59	7.93	50.73-unst	93.33	-0.111	Plasma membrane
CreCNGC17	Cre4g_025,000.1	III	5	4	28,114,436	28,119,138	-	723	83,242.23	9.34	41.19-unst	91.43	-0.188	Plasma membrane
	Cre2g_027,400.1	III	7	2	27,779,686	27,783,151	-	732	83,295.6	8.24	44.03-unst	91.81	-0.045	Plasma membrane
CreCNGC19	Cre5g_019,620.1	IV-A	4	5	22,012,270	22,033,591	-	777	89,294.76	9.43	46.42-unst	86.34	-0.215	Plasma membrane
C. grandis CNGCs														

(Continued on following page)

TABLE 2 (Continued) Physiochemical properties of Citrus Spp.

Gene Name	Protein id	Group	TM domains	Chr	Start	End	Strand	Protein length (AA)	Molecular weight (MW)	Isoelectric point (PI)	Instability index (II)	Aliphatic index (AI)	Grand average of hydrophathy (GRAVY)	Subcellular localization
CgCNGC1.1	Cg9g028350.1	I	5	9	38,716,748	38,721,456	-	936	107,162.85	9.43	48.3-unst	91.4	-0.121	Plasma membrane
CgCNGC1.2	Cg2g015410.1	I	1	2	19,778,512	19,781,575	+	299	34,216.96	9.22	47.85-unst	81.17	-0.285	Plasma membrane
CgCNGC1.3	Cg9g028420.1	I	5	9	38,786,148	38,792,072	+	962	109,694.28	8.76	42.63-unst	87.76	-0.201	Plasma membrane
CgCNGC1.4	Cg9g028570.1	I	5	9	39,116,699	39,120,252	+	677	78,034.42	8.65	39.24	94.91	-0.125	Plasma membrane
CgCNGC1.5	Cg9g028370.1	I	6	9	38,743,875	38,747,793	-	594	68,616.61	6.89	43.85-unst	98.95	0.018	Plasma membrane
CgCNGC1.6	Cg9g028360.1	I	11	9	38,727,773	38,740,199	-	1,289	147,329.05	8.7	39.32	98.98	0.066	Plasma membrane
CgCNGC1.7	Cg5g040810.1	I	4	5	46,534,174	46,549,973	-	1,075	121,375.2	7.06	55.13-unst	85.26	-0.238	Plasma membrane
CgCNGC2.1	Cg6g025480.1	IV-B	7	6	23,347,654	23,352,404	+	714	81,978.69	9.51	48.41-unst	93.1	-0.023	Plasma membrane
CgCNGC2.2	Cg6g025470.1	IV-B	6	6	23,334,786	23,338,688	-	668	76,781.88	9.47	52.18-unst	100.24	0.039	Plasma membrane
CgCNGC2.3	Cg9g020840.1	IV-B	4	9	30,004,781	30,012,835	+	729	83,109.01	6.06	38.86	101.09	-0.06	Plasma membrane
CgCNGC2.4	Cg9g024210.1	IV-B	5	9	34,705,798	34,717,552	+	817	93,522.72	6.74	35.61	96.4	-0.122	Plasma membrane
CgCNGC2.5	CgUng003220.1	IV-B	5	un	9,223,020	9,234,347	+	817	93,305.41	6.72	35.87	96.04	-0.13	Plasma membrane
CgCNGC2.6	Cg1g026270.1	IV-B	5	1	28,354,084	28,359,345	+	822	94,163.21	6.33	39.91	96.19	-0.166	Plasma membrane
CgCNGC4.1	Cg2g021840.1	IV-B	7	2	28,670,937	28,676,132	+	696	80,774.71	8.86	55.31-unst	89.21	-0.161	Plasma membrane
CgCNGC4.2	Cg3g002670.1	IV-B	5	3	4,661,834	4,672,023	-	834	95,075.26	7.35	34	99.74	-0.08	Plasma membrane
CgCNGC4.3	Cg4g003380.1	IV-B	5	4	3,087,474	3,110,776	-	1,020	115,444.86	6.33	47.72-unst	86.18	-0.232	Plasma membrane
CgCNGC4.4	Cg2g044770.1	IV-B	6	2	51,339,028	51,343,678	+	780	89,204.05	6.22	45.62-unst	90.47	-0.231	Plasma membrane
CgCNGC4.5	Cg4g002860.1	IV-B	5	4	2,629,924	2,633,950	+	885	99,323.22	7.62	44.8-unst	98.17	-0.122	Plasma membrane
CgCNGC4.6	Cg4g007830.1	IV-B	5	4	8,156,335	8,162,186	+	884	99,796.39	7.57	37.6	95.37	-0.155	Plasma membrane
CgCNGC5	Cg4g024210.1	II	5	4	28,735,763	28,743,584	+	734	84,009.72	9.04	49.85-unst	87.56	-0.171	Plasma membrane
CgCNGC7	Cg1g021430.1	II	5	1	19,715,772	19,722,167	-	747	85,912.18	9.25	46.4-unst	93.82	-0.137	Plasma membrane
CgCNGC8	Cg1g021420.1	II	5	1	19,706,850	19,712,083	-	749	86,209.43	9.22	50.26-unst	86.28	-0.189	Plasma membrane
CgCNGC10	Cg9g028390.1	I	5	9	38,755,211	38,760,218	-	710	81,642.58	9.21	46.82-unst	88.98	-0.134	Plasma membrane
Cg8g020040.1	Cg8g020040.1	III	7	8	17,731,791	17,735,688	+	733	83,844.22	9.61	45.47-unst	94.69	-0.153	Plasma membrane
CgCNGC15.1	Cg8g020050.1	III	5	8	17,741,847	17,745,309	+	698	80,206.9	9.3	51.75-unst	92.18	-0.148	Plasma membrane
CgCNGC15.2	Cg6g001850.2	III	6	6	3,649,106	3,652,936	+	705	81,198.2	9.21	52.81-unst	90.43	-0.103	Plasma membrane
CgCNGC15.3	Cg5g004760.1	III	4	5	3,321,460	3,324,100	+	604	69,207.65	7.93	50.59-unst	93.81	-0.102	Plasma membrane
CgCNGC16	Cg4g022550.1	III	5	4	26,987,542	26,992,837	-	725	83,522.38	9.35	41.65-unst	90.64	-0.213	Plasma membrane
CgCNGC18	Cg2g006290.1	III	7	2	5,624,043	5,627,541	+	732	83,366.68	8.38	44.03-unst	91.53	-0.053	Plasma membrane
CgCNGC19	Cg8g017160.1	IV-A	6	8	14,510,599	14,531,413	-	775	89,042.58	9.52	45.27-unst	86.69	-0.222	Plasma membrane
A. buxfolia CNGCs														
AbuCNGC1.1	Abu9g_022,130.1	I	5	9	27,069,259	27,073,875	-	939	107,083.9	9.52	47.33-unst	93.51	-0.11	Plasma membrane
AbuCNGC1.2	Abu2g_018,710.2	I	6	2	16,588,226	16,593,034	-	661	76,601.95	9.5	46.36-unst	94.09	-0.034	Plasma membrane
AbuCNGC1.3	Abu2g_018,830.1	I	1	2	16,897,414	16,899,525	-	286	33,628.85	9.7	41.71-unst	84.81	-0.31	Plasma membrane

(Continued on following page)

TABLE 2 (Continued) Physiochemical properties of *Citrus Spp.*

Gene Name	Protein id	Group	TM domains	Chr	Start	End	Strand	Protein length (AA)	Molecular weight (MW)	Isoelectric point (PI)	Instability index (II)	Aliphatic index (AI)	Grand average of hydrophathy (GRAVY)	Subcellular localization
AbuCNGC1.4	Abu8g_000,710.1	I	4	8	704,278	706,789	+	522	60,395.7	8.92	51.94-unst	92.61	-0.163	Plasma membrane
	Abu9g_022,350.5	I	3	9	27,365,334	27,375,225	+	557	63,987.2	7.85	39.53	98.11	0.042	Plasma membrane
AbuCNGC1.5														
	Abu9g_022,190.1	I	6	9	27,159,605	27,165,397	+	969	110,649.32	8.54	46.29-unst	88.73	-0.19	Plasma membrane
AbuCNGC1.6														
	Abu9g_022,320.1	I	5	9	27,342,484	27,349,932	+	673	77,463.98	8.77	38.57	94.9	-0.103	Plasma membrane
AbuCNGC1.7														
	Abu9g_022,150.1	I	12	9	27,113,191	27,121,549	-	1,181	136,159.61	8.58	39.59	94.56	0.037	Plasma membrane
AbuCNGC1.8														
	Abu9g_022,140.1	I	11	9	27,095,048	27,108,466	-	1,335	152,436.23	8.58	39.62	100.53	0.092	Plasma membrane
AbuCNGC1.9														
	Abu6g_000,500.2	IV-B	6	6	474,996	478,912	+	668	76,594.54	9.36	51.29-unst	98.79	0.036	Plasma membrane
AbuCNGC2.1														
	Abu9g_015,870.2	IV-B	5	9	21,464,048	21,475,242	+	814	93,256.41	6.34	38.23	97.71	-0.113	Plasma membrane
AbuCNGC2.2														
	Abu1g_022,970.1	IV-B	5	1	30,308,320	30,313,480	+	822	94,449.46	6.02	40.74-unst	95.94	-0.178	Plasma membrane
AbuCNGC2.3														
	Abu4g_000,580.1	IV-B	7	4	929,289	934,439	-	693	80,470.5	9.02	55.04-unst	89.31	-0.162	Plasma membrane
AbuCNGC4.1														
	Abu3g_004,740.1	IV-B	3	3	8,031,152	8,078,661	-	886	100,067.3	8.53	34.86	92.02	-0.243	Plasma membrane
AbuCNGC4.2														
	Abu4g_010,210.1	IV-B	6	4	15,460,939	15,467,104	+	640	73,120.55	7.35	35.41	100.97	-0.021	Plasma membrane
AbuCNGC4.3														
	Abu2g_002,010.1	IV-B	5	2	1,267,031	1,275,718	-	785	89,829.7	7.01	38.86	88.55	-0.256	Plasma membrane
AbuCNGC4.4														
	Abu4g_010,650.1	IV-B	5	4	15,888,308	15,892,727	-	888	99,850.72	8.12	43.69-unst	96.84	-0.153	Plasma membrane
AbuCNGC4.5														
	Abu4g_007,510.2	IV-B	5	4	13,188,706	13,194,715	-	884	99,691.1	6.79	38.84	94.81	-0.167	Plasma membrane
AbuCNGC4.6														
	AbuCNGC5	Abu4g_014,390.1	II	5	4	19,300,156	19,309,549	-	732	83,809.62	9.16	50.51-unst	87.93	-0.163
AbuCNGC7														
	Abu1g_017,150.1	II	5	1	17,212,858	17,217,425	-	747	85,984.47	9.39	46.79-unst	94.49	-0.14	Plasma membrane
AbuCNGC8														
	Abu1g_017,140.1	II	5	1	17,201,248	17,206,481	-	749	86,207.42	9.11	50.72-unst	86.14	-0.179	Plasma membrane
AbuCNGC10														
	Abu9g_022,160.1	I	5	9	27,123,220	27,128,187	-	710	81,674.45	9.01	47.61-unst	89.8	-0.139	Plasma membrane
AbuCNGC13														
	Abu5g_004,430.1	I	4	5	3,240,422	3,244,666	+	723	83,110.2	8.86	49.86-unst	88.74	-0.154	Plasma membrane
AbuCNGC15.1														
	Abu8g_008,400.1	III	6	8	14,287,103	14,290,189	+	632	71,188.48	9.2	43.22-unst	98.68	0.013	Plasma membrane
AbuCNGC15.2														
	Abu8g_008,410.1	III	5	8	14,297,412	14,301,227	+	698	80,160.93	9.33	51.8-unst	92.88	-0.148	Plasma membrane
AbuCNGC15.3														
	Abu6g_018,420.1	III	6	6	15,292,506	15,295,954	-	711	81,741.94	9.29	53.96-unst	92.85	-0.087	Plasma membrane
AbuCNGC16.1														
	Abuscaffold_270_000,010.1	III	scaffold_270	408	2,260	+	473	54,718.45	6.66	56.95-unst	83.52	-0.325	Plasma membrane	

(Continued on following page)

TABLE 2 (Continued) Physiochemical properties of Citrus Spp.

Gene Name	Protein id	Group	TM domains	Chr	Start	End	Strand	Protein length (AA)	Molecular weight (MW)	Isoelectric point (PI)	Instability index (II)	Aliphatic index (AI)	Grand average of hydrophathy (GRAVY)	Subcellular localization
AbuCNGC16.2	Abu5g_041,550.1	III	1	5	50,800,866	50,803,218	-	482	55,785.78	6.62	55.91-unst	84.18	-0.298	Plasma membrane
	Abu4g_015,360.1	III	5	4	20,050,861	20,056,336	+	724	83,556.57	9.38	39.93	91.7	-0.209	Plasma membrane
AbuCNGC17														
AbuCNGC18	Abu2g_024,930.1	III	7	2	25,802,387	25,806,145	-	732	83,306.53	8.24	45.67-unst	90.6	-0.063	Plasma membrane
	Abu5g_025,960.1	IV-A	4	5	29,492,412	29,513,177	+	777	89,414.99	9.41	43.36-unst	87.98	-0.211	Plasma membrane
AbuCNGC19														
P. trifoliata CNGCs														
PtCNGC1.1	Pt9g018530.1	I	5	9	25,015,230	25,020,827	-	973	110,771.04	9.37	48.94-unst	93.85	-0.11	Plasma membrane
PtCNGC1.2	Pt9g018460.1	I	7	9	25,083,546	25,090,484	+	1,032	117,365.49	8.68	44.31-unst	91.9	-0.174	Plasma membrane
PtCNGC1.3	Pt9g018430.1	I	9	9	25,179,672	25,187,070	+	1,250	143,552.89	8.45	42.96-unst	93.27	-0.072	Plasma membrane
PtCNGC1.4	Pt9g018500.1	I	11	9	25,043,857	25,051,963	-	1,182	136,323.92	8.82	44.89-unst	93.67	0	Plasma membrane
PtCNGC1.5	Pt9g018510.1	I	8	9	25,029,556	25,039,658	-	1,024	116,524.29	8.57	36.37	98.81	0.144	Plasma membrane
PtCNGC2.1	Pt6g003400.1	IV-B	7	6	444,230	489,519	-	713	81,948.83	9.54	47.3-unst	94.73	0.003	Plasma membrane
PtCNGC2.2	PtUn034160.1	IV-B	7	un	66,243,252	66,247,985	+	714	82,071.86	9.54	48.32-unst	92.96	-0.019	Plasma membrane
PtCNGC2.3	Pt6g003390.1	IV-B	6	6	493,761	500,211	+	709	81,219.32	9.6	49.75-unst	102.01	0.067	Plasma membrane
PtCNGC2.4	Pt9g003410.1	IV-B	5	6	476,681	480,770	+	664	76,206.35	9.53	50.54-unst	101.15	0.037	Plasma membrane
PtCNGC2.5	Pt7g003350.3	IV-B	3	7	3,976,926	3,995,696	-	936	106,962.74	6.71	43.4-unst	84.49	-0.396	Plasma membrane, cytoplasmic, nuclear
PtCNGC2.6	Pt9g012630.1	IV-B	5	9	14,547,685	14,559,074	+	816	93,222.34	6.86	35.94	95.68	-0.13	Plasma membrane
PtCNGC4.1	Pt1g012590.1	IV-B	7	1	17,530,718	17,536,236	+	699	81,296.24	8.69	58.11-unst	89.24	-0.177	Plasma membrane
PtCNGC4.2	PtUn009010.1	IV-B	5	un	15,359,017	15,369,473	-	832	94,926	7.59	34.09	99.39	-0.1	Plasma membrane
PtCNGC4.3	Pt1g005510.1	IV-B	6	1	2,792,308	2,798,621	-	633	72,391.96	8.98	35.92	101.65	0.005	Plasma membrane
PtCNGC4.4	Pt2g029140.1	IV-B	5	2	29,148,344	29,152,343	+	790	90,218.22	6.62	43.24-unst	89.1	-0.215	Plasma membrane
PtCNGC4.5	Pt1g006070.1	IV-B	5	1	2,340,521	2,345,295	+	887	99,790.77	7.92	44.34-unst	98.6	-0.124	Plasma membrane
PtCNGC4.6	Pt1g002920.1	IV-B	5	1	5,000,257	5,006,083	+	884	99,733.32	6.81	39.2	96.14	-0.141	Plasma membrane
PtCNGC5	Pt1g019810.1	II	5	1	26,803,045	26,810,973	+	733	83,748.49	9.13	50.29-unst	88.36	-0.16	Plasma membrane
PtCNGC7	Pt7g005810.1	II	4	7	8,049,190	8,059,979	+	1,061	121,091.84	9.18	44.54-unst	93.62	-0.156	Plasma membrane
PtCNGC8	Pt7g005820.1	II	5	7	8,063,471	8,068,726	+	749	86,208.44	9.26	50-unst	86.27	-0.185	Plasma membrane
PtCNGC10	Pt9g018490.1	I	5	9	25,053,675	25,058,703	-	710	81,507.37	9.09	46.31-unst	90.35	-0.115	Plasma membrane
PtCNGC13	Pt3g033630.1	I	5	3	40,975,639	40,980,331	-	724	83,351.69	9.14	52.09-unst	89.97	-0.165	Plasma membrane
PtCNGC14	Pt1g001460.1	III	1	1	615,563	619,051	+	575	66,098.6	8.35	46.52-unst	82.74	-0.333	Plasma membrane
PtCNGC15.1	Pt8g007980.1	III	6	8	6,803,620	6,807,501	+	686	78,923.15	9.43	51.85-unst	89.21	-0.234	Plasma membrane
PtCNGC15.2	Pt8g007990.1	III	6	8	6,812,971	6,817,286	+	696	80,231.95	9.31	50.7-unst	92.45	-0.157	Plasma membrane
PtCNGC15.3	Pt6g018010.1	III	6	6	14,936,563	14,940,184	-	711	81,804.94	9.29	53.44-unst	89.82	-0.122	Plasma membrane
PtCNGC16	Pt3g005720.1	III	4	3	3,690,317	3,693,148	+	604	69,139.53	7.93	50.71-unst	93.33	-0.109	Plasma membrane
PtCNGC17	Pt1g020720.1	III	5	1	26,189,592	26,195,161	-	725	83,315.1	9.16	40.71-unst	90.77	-0.194	Plasma membrane
PtCNGC18	Pt2g007780.1	III	7	2	5,133,162	5,136,635	+	732	83,451.7	8.24	43.42-unst	91	-0.068	Plasma membrane
PtCNGC19	Pt3g017600.1	IV-A	4	3	19,663,677	19,685,454	-	777	89,598.1	9.43	45.22-unst	85.58	-0.237	Plasma membrane

TABLE 3 Ka, Ks, Ka/Ks values calculated for homologous gene pairs of *A. thaliana* and *C. sinensis*.

Gene 1	Gene 2	Ka	Ks	Ka/Ks	Duplication time (MYA)	Duplication Type
AtCNGC3	AtCNGC11	0.4516	0.9547	0.473,028,176	72.76,676,829	Tandem
AtCNGC3	AtCNGC13	0.4489	1.0099	0.444,499,455	76.97,408,537	Segmental
AtCNGC5	AtCNGC8	0.4158	0.824	0.50,461,165	62.80,487,805	Segmental
AtCNGC6	AtCNGC7	0.3829	0.6195	0.618,079,096	47.2,179,878	Segmental
AtCNGC6	AtCNGC9	0.1566	0.3842	0.407,600,208	29.28,353,659	Segmental
AtCNGC7	AtCNGC8	0.1359	0.3399	0.399,823,477	25.9,070,122	Tandem
AtCNGC10	AtCNGC13	0.192	0.2735	0.702,010,969	20.84,603,659	Segmental
AtCNGC11	AtCNGC12	0.0167	0.0504	0.331,349,206	3.841,463,415	Tandem
AtCNGC14	AtCNGC17	0.6632	1.1835	0.560,371,779	90.20,579,268	Segmental
AtCNGC19	AtCNGC20	0.2291	0.2634	0.869,779,803	20.07,621,951	Tandem
CsCNGC1.1	CsCNGC1.8	1.59	2.0937	0.759,421,121	159.5,807,927	Tandem
CsCNGC1.8	CsCNGC1.9	1.8165	1.7537	1.035,810,002	133.6,661,585	Tandem
CsCNGC2.1	CsCNGC2.2	0.6555	0.8614	0.760,970,513	65.6,554,878	Tandem
CsCNGC2.3	CsCNGC2.4	0.0135	0.0238	0.567,226,891	1.81,402,439	Segmental
CsCNGC2.3	CsCNGC2.5	0.0343	0.0118	2.906,779,661	0.899,390,244	Segmental
CsCNGC2.3	CsCNGC2.6	0.6756	0.8021	0.842,288,991	61.13,567,073	Segmental
CsCNGC2.4	CsCNGC2.5	0.0343	0.0359	0.955,431,755	2.736,280,488	Segmental
CsCNGC2.4	CsCNGC2.6	0.6828	0.7726	0.883,769,091	58.88,719,512	Segmental
CsCNGC2.5	CsCNGC2.6	0.6592	0.8374	0.787,198,471	63.82,621,951	Segmental
CsCNGC7	CsCNGC8	0.2583	0.2099	1.230,585,993	15.99,847,561	Tandem

group as compared to previously reported CNGC members in other plants.

3.4 Gene structure and conserved motif analysis

Gene structure analysis revealed that members from each subspecies are having their own set of exons and introns. Exons that belong to group I of CsCNGC ranged from 6 to 17 while exons that belong to group I of AtCNGCs ranged from 7 to 9. Exons that belong to group II of CsCNGC were 7 while exons that belong to group II of AtCNGCs ranged from 6 to 9. Exons that belong to group III of CsCNGC and AtCNGC ranged from 6 to 7. Exons that belong to group IV-A of CsCNGC were 12 while exons that belong to group IV-A of AtCNGC ranged from 10 to 11. Exons that belong to group IV-B of CsCNGC ranged from 7 to 14 while exons that belong to group IV-B of AtCNGC ranged from 8 to 9.

Ten motifs were identified in CsCNGCs and named motif 1 to motif 10. Motif 1 represents a combination of the Calmodulin binding motif (CaMB) and motif for the IQ domain. Motif 6 represents the hinge motif, while motif 9 represents the PBC motif. Both these motifs together constitute the cNMP/Cyclic nucleotide-binding domain (CNBD). Other motifs are responsible for unknown functions.

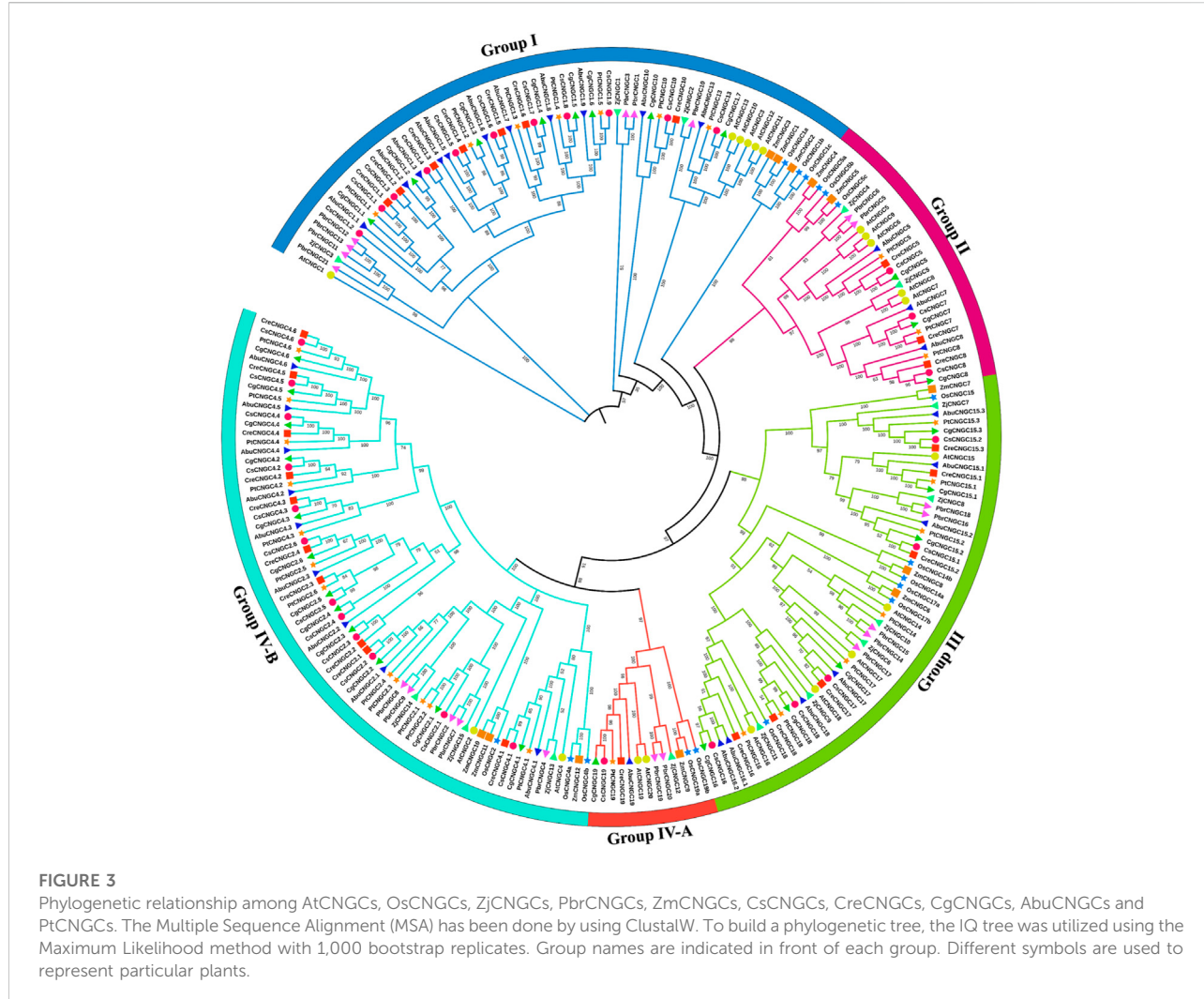
The gene structure and logo of conserved motifs of *C. Sinensis* are given in (Figure 4, Supplementary Figure S5).

Group I of CreCNGCs contained exons ranging from 4 to 17, 5 to 7 exons exist in group II of CreCNGC, exons that exist in group III of CreCNGCs were 6–8, and 12 exons were present in group IV-A of CreCNGCs and 7 to 13 exons were present in group IV-B of CreCNGCs. Motif 5 represents the PBC motif and motif 2 contains the hinge motif, CaMB motif, and motif for the IQ domain. Other motifs were representing motifs of unknown function (Supplementary Figures S6A,B).

Group I of CgCNGC contained 4 to 17 exons, group II of CgCNGC contained 7 exons, group III of CgCNGC contained 6 to 8, and group IV-A of CgCNGC contained 12 exons and group IV-B of CgCNGC contained 7 to 14 exons. Motif 3 represents a combination of CaMB motif and motif for IQ-domain, motif 5 represents hinge region motif and motif 7 represents PBC motif (Supplementary Figures S7A,B).

In AbuCNGC exons of group I were ranging from 4 to 18, exons of group II were ranging from 6 to 7, exons of group III were ranging from 4 to 7, exons of group IV-A 12, and exons of group IV-B were ranging from 7 to 14. Motif 3 represents a combination of CaMB motif and motif for IQ-domain, motif 8 represents PBC motif and motif 2 contains hinge motif (Supplementary Figures S8A,B).

Exon number for group I of PtCNGC ranged from 6 to 16, exon number for group II of PtCNGC ranged from 7 to 12, exon number for group III of PtCNGC ranged from 6 to 9, and exon



number for group IV-A of *PtCNGC* were 12 and exon number for group IV-B of *PtCNGC* ranged from 7 to 18. Motif 2 represents the CaMB motif and motif for the IQ domain, motif 3 represents the Cyclic nucleotide-binding domain that contains both PBC and hinge motif. The representation of motifs and logo of conserved motifs of *P. trifoliata* is displayed (Supplementary Figures S9A,B).

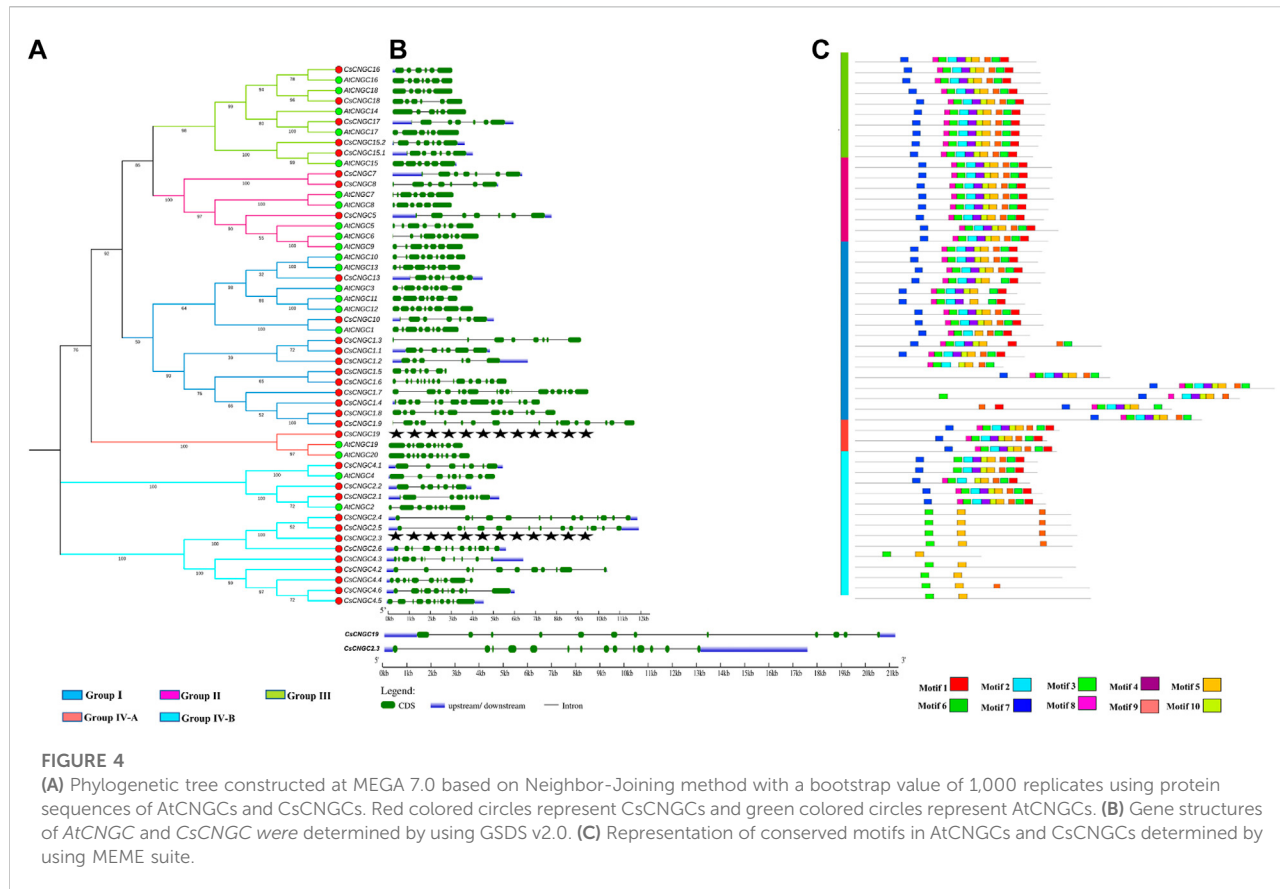
Hence, the PBC motif, hinge motif, CaMB motif, and motif for the IQ domain was conserved in 5 Citrus *Spp.* indicating that genes identified in the current study are truly CNGC genes.

3.5 Chromosomal mapping

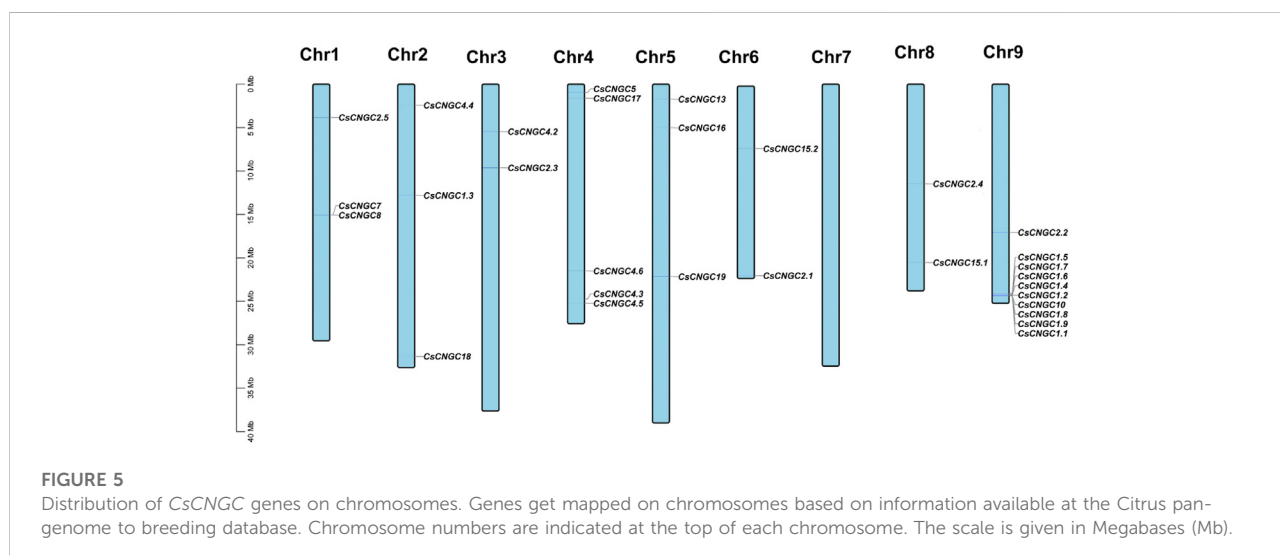
In *C. sinensis* 32 genes were distributed unevenly on 8 out of 9 chromosomes. *C. sinensis* had maximum genes (10) at

chromosome 9, minimum genes (2) at chromosomes 3, 6, and 8, and there was no gene on chromosome 7. The distribution of *CsCNGC* on chromosomes is given in (Figure 5).

27 genes were mapped unevenly at 8 out of 9 chromosomes in *C. reticulata*. In *C. reticulata* maximum genes (8) were present at chromosome 9, minimum genes (1) were present at chromosome 3, and no gene was present at chromosome 7 (Supplementary Figure S10). In *C. grandis* chromosome 9 carried maximum genes (8), chromosome 3 carried minimum genes (1), and none of the genes was present on chromosome 7 (Supplementary Figure S11). In *A. buxfolia* chromosome 9 contained maximum genes (8), chromosome 3 contained minimum genes (1) and none of the genes was present on chromosome 7 (Supplementary Figure S12). In *P. trifoliata* there were maximum genes (7) present at chromosome 9 and chromosome 1, there were minimum genes (2) present at chromosomes 2 and 8 and there was no

**FIGURE 4**

(A) Phylogenetic tree constructed at MEGA 7.0 based on Neighbor-Joining method with a bootstrap value of 1,000 replicates using protein sequences of AtCNGCs and CsCNGCs. Red colored circles represent CsCNGCs and green colored circles represent AtCNGCs. (B) Gene structures of AtCNGC and CsCNGC were determined by using GSDS v2.0. (C) Representation of conserved motifs in AtCNGCs and CsCNGCs determined by using MEME suite.

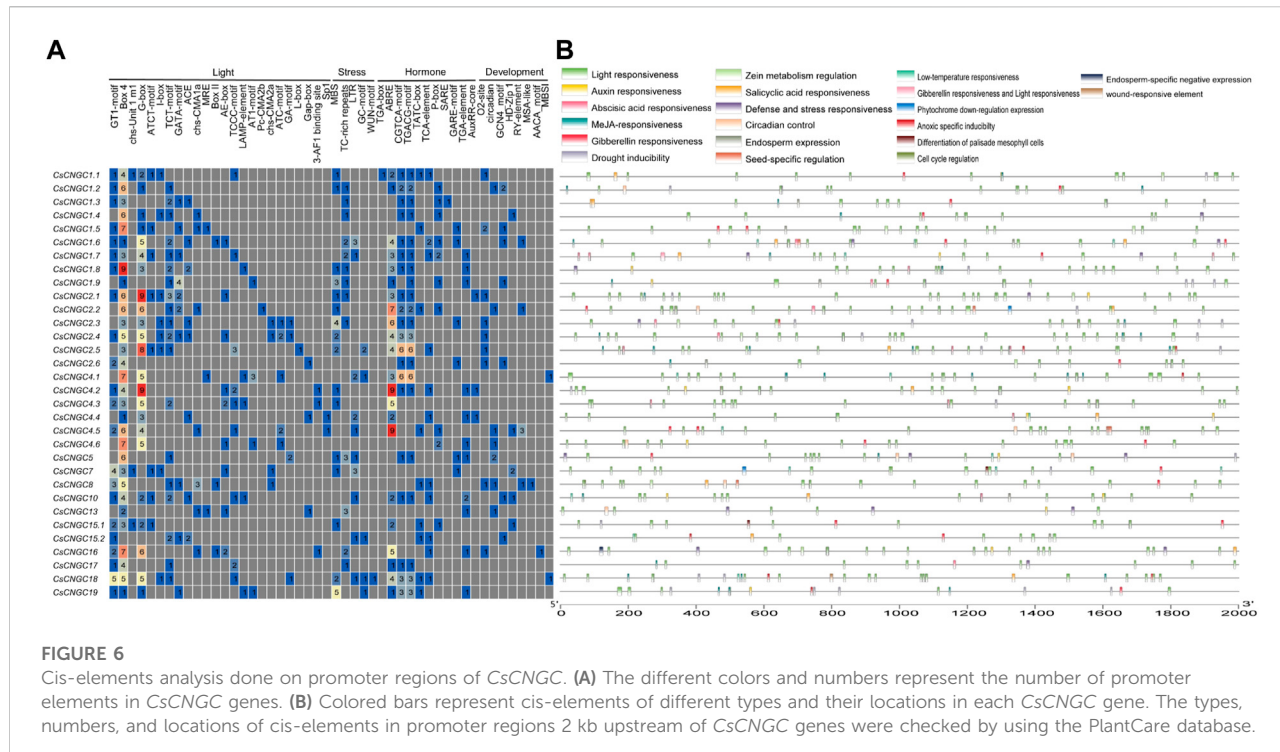
**FIGURE 5**

Distribution of CsCNGC genes on chromosomes. Genes get mapped on chromosomes based on information available at the Citrus pan-genome to breeding database. Chromosome numbers are indicated at the top of each chromosome. The scale is given in Megabases (Mb).

gene present at chromosomes 4 and 5 (Supplementary Figure S13). Thus, it can be inferred that CNGC genes were distributed unevenly at 8 out of 9 chromosomes in Citrus *Spp.* except for *P. trifoliata* in which genes were distributed at 7 out of 9 chromosomes.

3.6 Gene duplication events

The duplication pairs resulting from segmental duplication in *C. sinensis* include CsCNGC2.3/CsCNGC2.4, CsCNGC2.3/CsCNGC2.5, CsCNGC2.3/CsCNGC2.6, CsCNGC2.4/CsCNGC2.5,

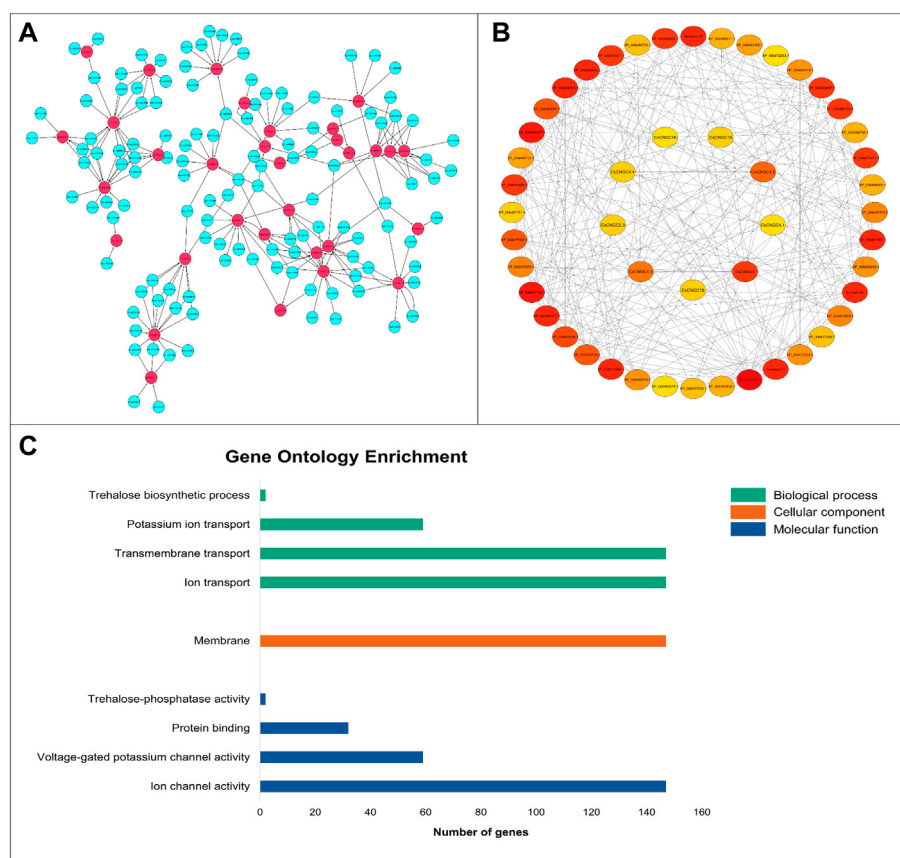


CsCNGC2.4/CsCNGC2.6, CsCNGC2.5/CSCNGC2.6. The gene pairs that were tandemly duplicated in *C. sinensis* include *CsCNGC1.1/CsCNGC1.8*, *CsCNGC1.8/CsCNGC1.9*, *CsCNGC2.1/CsCNGC2.2*, *CsCNGC7/CsCNGC8*. The gene pairs of *A. thaliana* CNGCs that were tandemly duplicated include *AtCNGC3/AtCNGC11*, *AtCNGC7/AtCNGC8*, *AtCNGC11/AtCNGC12*, *AtCNGC19/AtCNGC20*. The gene pairs of *A. thaliana* CNGCs that were segmentally duplicated include *AtCNGC3/AtCNGC13*, *AtCNGC5/AtCNGC8*, *AtCNGC6/AtCNGC7*, *AtCNGC6/AtCNGC9*, *AtCNGC10/AtCNGC13*, *AtCNGC14/AtCNGC17*. Genes were duplicated segmentally as well as tandemly in both *C. sinensis* and *A. thaliana* indicating that both segmental and tandem duplications are involved in the expansion of CsCNGC genes. Moreover, the rate of non-synonymous substitutions (Ka), rate of synonymous substitutions (Ks), Ka/Ks, and duplication time (MYA) were calculated. The Ks of 6 segmental duplicates in *C. sinensis* ranged from 0.0118 to 0.8374, also Ks of 4 tandem duplicates ranged from 0.2099 to 2.0937, and duplication time of both segmental and tandem duplicates ranged from 0.89 MYA to 159 MYA. The Ka/Ks value of *CsCNGC1.1/CsCNGC1.8*, *CsCNGC2.1/CsCNGC2.2*, *CsCNGC2.3/CsCNGC2.4*, *CsCNGC2.3/CsCNGC2.6*, *CsCNGC2.4/CsCNGC2.5*, *CsCNGC2.4/CsCNGC2.6*, *CsCNGC2.5/CSCNGC2.6* was less than 1 indicating the occurrence of purifying selection in duplication of these genes. The Ka/Ks value of *CsCNGC1.8/CsCNGC1.9*, *CsCNGC2.3/CsCNGC2.5*, *CsCNGC7/CsCNGC8* was greater than 1 indicating the role of positive selection in duplication of these genes. Similarly, the Ks

of 6 segmental duplicates in *A. thaliana* ranged from 0.2735 to 1.1835, and also the Ks value of 4 tandem duplicates ranged from 0.0504 to 0.9547, and the duplication time of both segmental and tandem duplicates ranged from 3.84 MYA to 90.20 million years ago (MYA) (Table 3).

In *C. recticulata* gene pairs that were the product of segmental duplication include *CreCNGC2.2/CreCNGC2.4*, *CreCNGC2.3/CreCNGC2.4*. The gene pairs that were the product of tandem duplication include *CreCNGC2.2/CreCNGC2.3*, *CreCNGC7/CreCNGC8*, and *CreCNGC15.1/CreCNGC15.2*. Altogether 5 gene pairs were duplicated and among these 3 gene pairs were tandemly duplicated indicating the role of tandem duplication in the expansion of CreCNGC genes. The Ks of 2 segmental duplicates in *C. recticulata* were 0.50, also Ks of 3 tandem duplicates ranged from 0.05 to 0.56, and the duplication time of both segmental and tandem duplicates ranged from 4.23 MYA to 42.74 MYA. The Ka/Ks value of CreCNGCs was less than 1 indicating that purifying selection has occurred in this duplication event (Supplementary Table S3).

The segmentally duplicated gene pairs of *C. grandis* include *CgCNGC2.3/CgCNGC2.5*, *CgCNGC2.3/CgCNGC2.6*, *CgCNGC2.4/CgCNGC2.5*, *CgCNGC2.4/CgCNGC2.6*, *CgCNGC2.5/CgCNGC2.6*. The tandemly duplicated gene pairs include *CgCNGC1.5/CgCNGC1.6*, *CgCNGC2.1/CgCNGC2.2*, *CgCNGC2.3/CgCNGC2.4*, *CgCNGC7/CgCNGC8*, *CgCNGC15.1/CgCNGC15.2*. Overall, 10 gene pairs were duplicated and out of these 5 gene pairs were segmentally duplicated and 5 were tandemly duplicated indicating the equal contribution of both events in the expansion

**FIGURE 7**

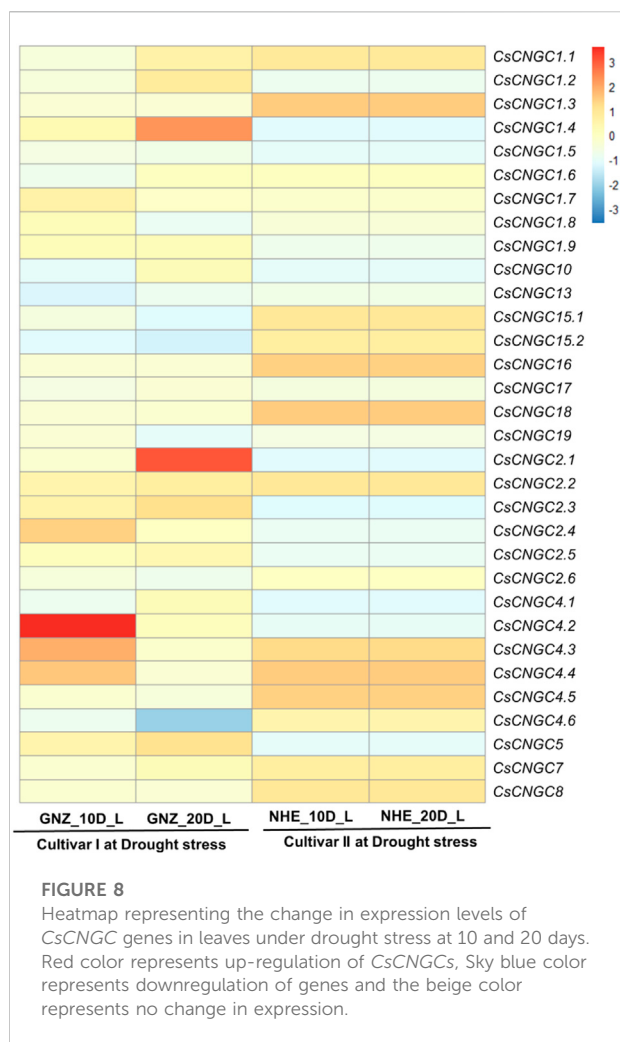
(A) Network representation of regulatory association among miRNAs and CsCNGCs. The network has been constructed by using Cytoscape. The miRNAs involved in regulating CsCNGCs are colored blue. CsCNGC genes are colored red and black colored lines represent the regulatory relationship. **(B)** Network showing the interactions among CsCNGCs and other protein members predicted using STRING database. The nodes are colored according to the degree of interactions. The red color is showing the protein has a higher level of connectivity with other members, orange-colored nodes have a relatively lesser level of interactions with other proteins while yellow-colored nodes have the least interactions with other proteins. **(C)** Gene ontology enrichment statistics graph, the green color bar represents biological processes, the orange color bar represents a cellular component, and the blue color bar represents the molecular function.

of CgCNGC genes. The Ks of 5 segmental duplicates in *C. grandis* ranged from 0.03 to 0.74, also Ks of 5 tandem duplicates ranged from 0.02 to 0.44, and the duplication time of both segmental and tandem duplicates ranged from 1.71 MYA to 69.20 MYA. The Ka/Ks value of five gene pairs was less than 1 indicating the role of purifying selection in the duplication of these genes. The Ka/Ks value of four gene pairs was less than 1 indicating the role of purifying selection in the duplication of these gene pairs and one gene pair (*CgCNGC2.3/CgCNGC2.4*) greater than 1 indicating the role of positive selection in the duplication of this gene pair (Supplementary Table S3).

The gene pairs that were segmentally duplicated in *A. buxfolia* include *AbuCNGC1.2/CreCNGC1.7*, *AbuCNGC1.2/AbuCNGC1.9*, *AbuCNGC1.3/AbuCNGC1.7*, *AbuCNGC1.3/AbuCNGC1.9*, *AbuCNGC2.2/AbuCNGC2.3*. Tandemly duplicated gene pairs include *AbuCNGC1.1/AbuCNGC1.8*, *AbuCNGC1.1/AbuCNGC10*, *AbuCNGC1.8/AbuCNGC1.9*,

AbuCNGC7/AbuCNGC8. In total 9 gene pairs were duplicated and among these 5 gene pairs were segmentally duplicated and 4 were tandemly duplicated indicating the role of segmental duplication in the expansion of *AbuCNGC* genes. The Ks of 5 segmental duplicates in *A. buxfolia* ranged from 0.85 to 2.55, also Ks of 4 tandem duplicates ranged from 0.14 to 1.85, and the duplication time of both segmental and tandem duplicates ranged from 11.36 MYA to 195 MYA. The Ka/Ks value of eight gene pairs was less than 1 indicating the role of purifying selection in the duplication of these gene pairs. While the Ka/Ks value of only one gene pair (*AbuCNGC7/AbuCNGC8*) was greater than 1 indicating the role of positive selection in the duplication of this gene pair (Supplementary Table S3).

The duplicated gene pairs that arise from segmental duplication in *P. trifoliata* include *PtCNGC2.2/PtCNGC2.3*, *PtCNGC2.2/PtCNGC2.4*, *PtCNGC2.5/PtCNGC2.6*, *PtCNGC5*/



PtCNGC8. The gene pairs that arise from tandem duplication include *PtCNGC1.4/PtCNGC1.5*, *PtCNGC2.1/PtCNGC2.3*, *PtCNGC2.1/PtCNGC2.4*, *PtCNGC2.3/PtCNGC2.4*, *PtCNGC14/PtCNGC1*, *PtCNGC15.1/PtCNGC15.2*. A total of 10 gene pairs were duplicated and among them, 4 gene pairs were segmentally duplicated and 6 were tandemly duplicated indicating the role of tandem duplication in the expansion of *PtCNGC* genes. Moreover, the rate of non-synonymous substitutions (Ka), rate of synonymous substitutions (Ks), Ka/Ks, and duplication time (MYA) were calculated. The Ks of 4 segmental duplicates in *P. trifoliata* ranged from 1.09 to 1.83, also Ks of 6 tandem duplicates ranged from 0.06 to 1.45, and the duplication time of both segmental and tandem duplicates ranged from 4.81 MYA to 111.25 MYA. Mostly gene pairs have Ka/Ks value of less than 1 indicating the role of purifying selection in the duplication of these gene pairs. While the Ka/Ks value of *PtCNGC1.4/PtCNGC1.5* was greater than 1 indicating the role of positive selection in the duplication of this gene pair (Supplementary Table S3).

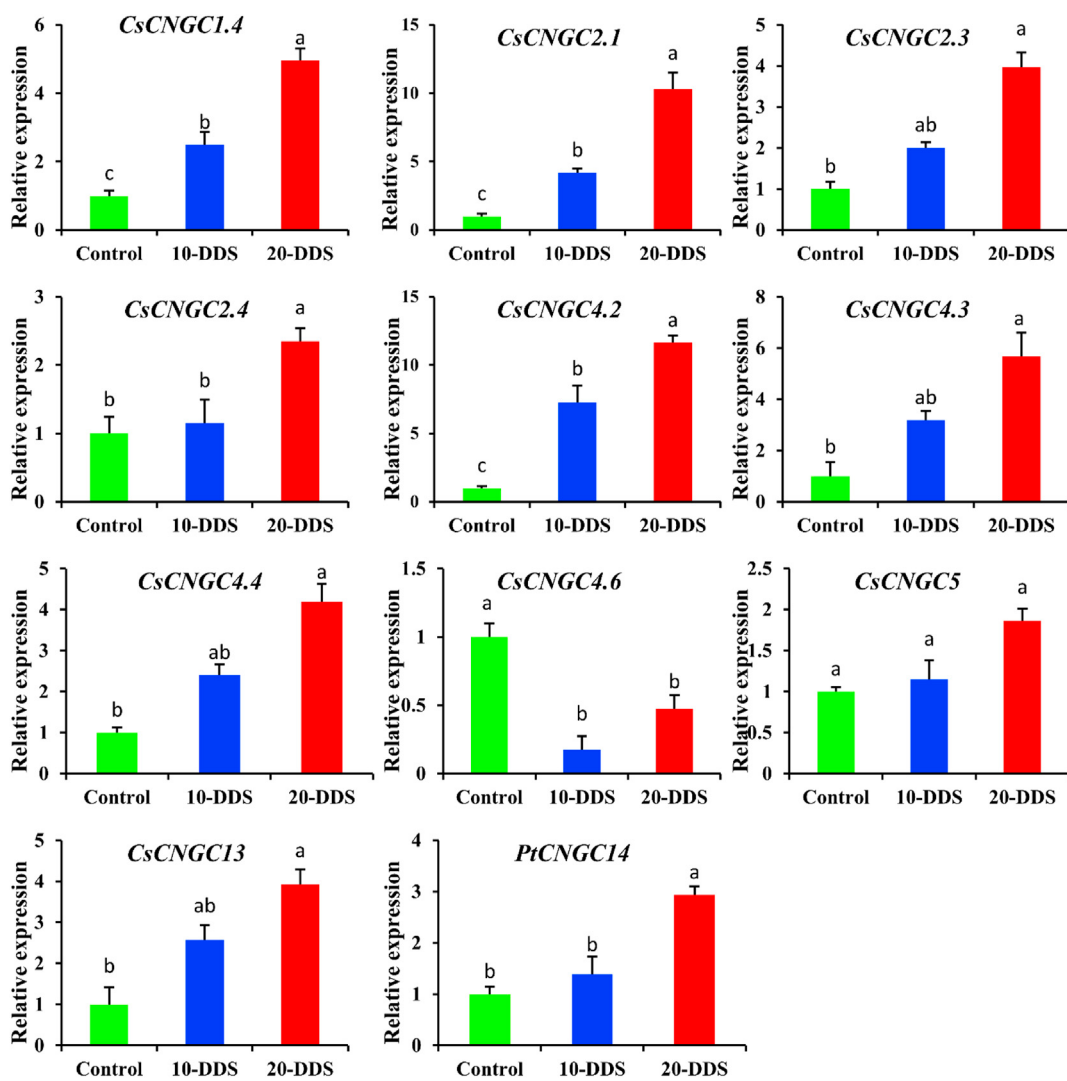
3.7 Cis-regulatory elements/promoter analysis of citrus *Spp.*

To clearly understand the role of cis-regulatory elements (CREs) in *CsCNGCs*, *CreCNGCs*, *CgCNGCs*, *AbuCNGCs*, and *PtCNGCs*, and the cis-elements in 2 kb upstream of TSS were identified. The results suggested that cis-elements of four types were identified namely, hormone-responsive, light-responsive, stress-related cis-elements, and plant development-related cis-elements in *CsCNGCs*, *CreCNGCs*, *CgCNGCs*, *AbuCNGCs*, *PtCNGCs*.

It was observed that cis-elements responsible for light responsiveness were present abundantly in *CsCNGCs*. Overall, 24 cis-elements responsible for light responsiveness were determined out of which Box 4 element was present in 31 *CsCNGCs*, GT1-motif and G box elements were present in 22 *CsCNGCs* and 23 *CsCNGCs* and others were present in very few CNGCs. Among 11 hormone-related cis-elements, the ABRE element was present in 22 *CsCNGCs*, the CGTCA motif and TGACG motifs were present in 20 *CsCNGCs*, and 21 *CsCNGCs*, TCA element, and TATC box were present in 9 *CsCNGCs* and 11 *CsCNGCs* and other hormone-related elements were present in very few *CsCNGCs*. Among 5 stress-related cis-elements, MBS element (drought inducible) was present in 16 *CsCNGCs*, TC-rich repeats element (defense responsive) was present in 13 *CsCNGCs* and LTR, GC motif, WUN motif was present in very few *CsCNGCs*. Out of 8 development-related cis-elements, GCN4_motif and circadian were present in 7 *CsCNGCs* and O2 site element was present in 9 *CsCNGCs* and others were present in very few *CsCNGCs*. The results demonstrate that *CsCNGCs* are involved in plant growth, development, and response to abiotic stress. The graphical representation of the location and types of cis-elements present in *CsCNGCs* is given in (Figure 6).

Cis-elements responsible for light responsiveness were present abundantly in *CreCNGCs*. Overall, 27 cis-elements responsible for light responsiveness were determined out of which Box4 was present in 25 *CreCNGCs*, G box was present in 22 *CreCNGCs*, and GT1 motif was present in 17 *CreCNGCs* and others were present in very few *CreCNGCs*. Among 10 hormone-related cis-elements, ABRE was present in 18 *CreCNGCs*, TGACG motif was present in 17 *CreCNGCs*, TCA element was present in 14 *CreCNGCs* and others were present in very few *CreCNGCs*. Among 4 stress-related cis-elements, LTR was present in 12 *CreCNGCs*, MBS was present in 10 *CreCNGCs*, TC-rich repeats element was present in 9 *CreCNGCs*, and GCmotif was present in 4 *CreCNGCs*. Out of 6 development-related cis-elements RY element, O2 site, and GCN4 motif were present in 6 *CreCNGCs* and others were present in very few *CreCNGCs* (Supplementary Figure S14).

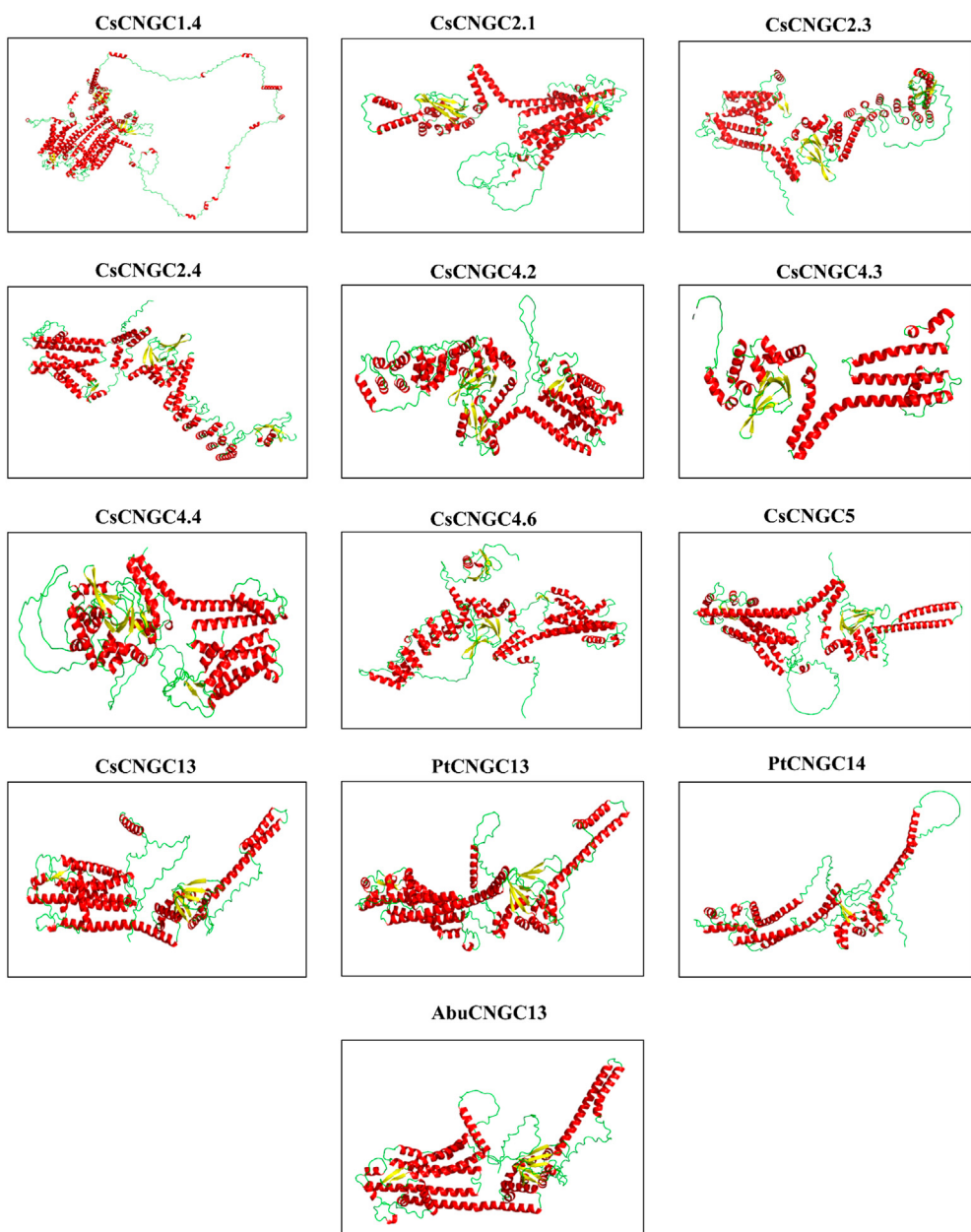
CgCNGCs also contained a number of light-responsive CREs. Overall, 24 cis-elements responsible for light responsiveness were determined out of which Box4 was present in 28 *CgCNGCs*, G

**FIGURE 9**

The graphs represent the qRT-PCR results of *CsCNGC* genes under drought stress. 10-DDS: 10 days of drought stress; 20-DDS: 20 days of drought. Each column represents the mean of three biological replicates. The least significant difference was applied to compare the difference between control and dissimilar drought stress levels at $p < 0.05$ (a, b, c).

box was present in 25 *CgCNGCs*, and GT1 motif was present in 22 *CgCNGCs* and others were present in very few *CgCNGCs*. Among 9 hormone-related cis elements ABRE was present in 23 *CgCNGCs*, CGTCA motif was present in 17 *CgCNGCs*, TGACG motif was present in 18 *CgCNGCs* and others were present in very few *CgCNGCs*. Among 5 stress-related cis-elements, MBS was present in 18 *CgCNGCs*, TC rich repeats element was present in 13 *CgCNGCs*, LTR was present in 11 *CgCNGCs* and others were present in very few *CgCNGCs*. Out of 7 development-related cis-elements, circadian was present in 5 *CgCNGCs*, GCN4 motif was present in 5 *CgCNGCs* and others were present in very few *CgCNGCs* (Supplementary Figure S15).

Cis-elements responsible for light responsiveness were present abundantly in *AbuCNGCs*. Overall, 24 cis-elements responsible for light responsiveness were determined out of which G box was present in 26 *AbuCNGCs*, Box 4 was present in 26 *AbuCNGCs*, and GT1 motif was present in 21 *AbuCNGCs*, TCT motif was present in 21 *AbuCNGCs* and others were present in very few *AbuCNGCs*. Among 9 hormone-related cis elements ABRE was present in 25 *AbuCNGCs*, TGACG motif and CGTCA motif were present in 16 *AbuCNGCs* and others were present in very few *AbuCNGCs*. Among 4 stress-related cis-elements, MBS was present in 17 *AbuCNGCs*, TC-rich repeats element was present in 10 *AbuCNGCs*, and others were present in very few

**FIGURE 10**

Predicted 3D structures of 12 CNGCs in *C. sinensis*, *A. buxfolia*, and *P. trifoliata* using Alphafold2. CsCNGC1.4 has been predicted by using tRosetta. Structures are displayed based on secondary structures. Spirals with red color represent alpha helices, wide arrows with yellow color represent beta sheets, and wires with green color represent the loops.

AbuCNGCs. Among 6 development-related cis-elements, circadian was present in 7 *AbuCNGCs*, O2 site was present in 5 *AbuCNGCs* and others were present in very few *AbuCNGCs* (Supplementary Figure S16).

Cis-elements responsible for light responsiveness were present abundantly in *PtCNGCs*. Overall, 24 cis-elements responsible for light responsiveness were determined out of which Box 4 was present in 25 *PtCNGCs*, G box was present

in 21 *PtCNGCs*, and GT1 motif was present in 18 *PtCNGCs* and others were present in very few *PtCNGCs*. Among 10 hormone-related cis-elements, ABRE was present in 22 *PtCNGCs*, CGTCA motif and TGACG motif were present in 17 *PtCNGCs* and others were present in very few *PtCNGCs*. Among 5 stress-related cis-elements, MBS was present in 17 *PtCNGCs*, TC-rich repeats element was present in 11 *PtCNGCs*, LTR was present in 7 *PtCNGCs* and others are present in very few *PtCNGCs*.

Among 7 development-related cis-elements, the RY element was present in 5 *PtCNGCs*, Circadian was present in 4 *PtCNGCs* and others were present in very few *PtCNGCs* (Supplementary Figure S17).

3.8 Pan-genome wide investigation of miRNAs targeting *CsCNGC* genes, protein-protein interaction, and gene ontology enrichment analysis

A total of 226 miRNAs were identified that targeted 32 *CsCNGCs* with expectation values ranging from 3.5 to 5 (Figure 7A). Only 1 miRNA was targeting *CsCNGC17* with an expectation value of 3.5, while 16 miRNAs were targeting *CsCNGC7* where all miRNAs have expectation value 5 except *Csi-miRN925* with expectation value 4.5, 10 miRNAs were targeting *CsCNGC1.1*, *CsCNGC2.3* and *CsCNGC2.4*, 4 miRNAs were targeting *CsCNGC1.2*, 9 miRNAs were targeting *CsCNGC1.3*, *CsCNGC10* and *CsCNGC13*, 11 miRNAs were targeting *CsCNGC1.4* and *CsCNGC1.8*, 5 miRNAs were targeting *CsCNGC1.5*, *CsCNGC15.1* and *CsCNGC2.1*, 7 miRNAs were targeting *CsCNGC1.6* and *CsCNGC18*, 13 miRNAs were targeting *CsCNGC1.7*, *CsCNGC16* and *CsCNGC8*, 3 miRNAs were targeting *CsCNGC1.9*, *CsCNGC15.2*, *CsCNGC2.6*, *CsCNGC4.3* and *CsCNGC5*, 2 miRNAs were targeting *CsCNGC4.1*, *CsCNGC4.2* and *CsCNGC19*, 6 miRNAs were targeting *CsCNGC2.2*, 8 miRNAs were targeting *CsCNGC2.5*, *CsCNGC4.4* and *CsCNGC4.5*, 6 miRNAs were targeting *CsCNGC4.6*. Detailed information related to these miRNAs regulated *CsCNGCs* is given in (Supplementary Table S4). Among these miRNAs, most of them were responsible for inhibiting the cleavage of target transcript while only a few were involved in inhibiting the translation of target genes.

The PPI network of *CsCNGC* proteins was constructed to reveal the interaction among these proteins and related proteins (Figure 7B) to understand their degree of connectivity and ultimately their functional relativity. It has been shown that the highest degree of connectivity was shown by syntaxin-121, a protein from the *C. sinensis* plant, which suggests that this protein may have some functional connectivity with the CNGC proteins. Similarly, other proteins including Membrin-11 and some vesicle-associated membrane proteins (acc: XP_006479311.1) also showed a higher degree of interaction. Among CNGC members, *CsCNGC4.6*, *CsCNGC4.2*, and *CsCNGC4.3* had higher interactions with other CNGC members as well as other related proteins. *CsCNGC2.3*, *CsCNGC4.1*, *CsCNGC4.4*, *CsCNGC16*, *CsCNGC18* and *CsCNGC19* had relatively lesser interactions. This level of connectivity reveals that these proteins might be involved in similar pathways thus regulating particular reactions and performing similar functions.

GO enrichment analyses were carried out on 5 Citrus *Spp.* to increase our understanding of the dynamic roles of CNGCs genes at the molecular level (Figure 7C; Supplementary Table S5). Based on GO analysis genes are classified into three major categories: biological process (BP), cellular component (CC), and molecular function (MF). Genes were mostly related to biological processes (4), molecular functions (4), and then cellular components (1). In the biological process, category 147 out of 150 genes were involved in ion transport (GO: 0,006,811) and transmembrane transport (GO:0,055,085), 59 genes were involved in potassium ion transport (GO: 0,006,813), and only 2 genes were involved in trehalose biosynthetic process (GO:0,005,992). In the cellular component category, 147 genes were mainly found in the membrane (GO:0,016,020) which is consistent with the subcellular localization prediction result. In the molecular function category, 147 genes were involved in ion channel activity (GO:0,005,216), 59 genes out of 150 are involved in voltage-gated potassium channel activity (GO:0,005,249), 32 genes in protein binding (GO:0,005,515), and only 2 genes were involved in the trehalose-phosphatase activity (GO: 0,004,805).

3.9 Expression profiling of *C. sinensis* under drought stress

RNA-Seq data analysis was performed for leaves sample of *C. sinensis* under drought stress in two cultivars namely Newhall navel (NHE) orange, and Gannanzao (GNZ) navel orange at 0,10 and 20 days. The results suggest that *CsCNGC2.1* and *CsCNGC1.4* were highly up-regulated in cultivar I (20 days) and *CsCNGC4.2* (10 days). *CsCNGC1.3*, *CsCNGC15.1*, *CsCNGC15.2*, *CsCNGC16* and *CsCNGC18* were slightly up-regulated in cultivar II (Figure 8).

CsCNGC1.1 was slightly up-regulated in cultivar I (20 days) and cultivar II. *CsCNGC2.2* was slightly up-regulated in both cultivars. *CsCNGC1.2* was slightly up-regulated in cultivar I (20 days). *CsCNGC1.7* was slightly up-regulated in cultivar I (10 days). *CsCNGC2.2* was slightly up-regulated in both cultivars. *CsCNGC2.3* was slightly up-regulated in cultivar I. *CsCNGC2.4* was slightly up-regulated in cultivar I (10 days). The increase in the expression level of these duplicated genes suggests that they not only evolved in number but in function also. *CsCNGC4.3* and *CsCNGC4.4* were slightly up-regulated in cultivar I (10 days) and cultivar II. *CsCNGC4.5* was slightly up-regulated in cultivar II. *CsCNGC7* and *CsCNGC8* were slightly upregulated in cultivar II. *CsCNGC4.6* was highly down-regulated in cultivar I (20 days) and slightly down-regulated in cultivar I (10 days). *CsCNGC1.4*, *CsCNGC1.5*, *CsCNGC1.9*, *CsCNGC2.1*, *CsCNGC2.3*, *CsCNGC2.4*, *CsCNGC2.5*, *CsCNGC2.6*, *CsCNGC4.2* and *CsCNGC5* were slightly down-regulated in cultivar II. *CsCNGC1.8* was slightly down-regulated in cultivar I

(20 days). Most of these genes have evolved through duplication which suggests that they are involved in the stress modulating process either by upregulating or downregulating their expression level. This change in their expression level may contribute to modulating stress response in drought stress as well. *CsCNGC10* was slightly down-regulated in cultivar I (10 days) and cultivar II. *CsCNGC13* was slightly down-regulated in both cultivars. *CsCNGC15.1*, *CsCNGC15.2*, *CsCNGC16* was slightly down-regulated in cultivar I. *CsCNGC19* was slightly downregulated in cultivar I (20 days). *CsCNGC1.1* and *CsCNGC1.2* in cultivar I (10 days), *CsCNGC1.3* and *CsCNGC1.5* in cultivar I, *CsCNGC1.6* in cultivar I (20 days) and cultivar II, *CsCNGC1.7* in cultivar I at (20 days) and cultivar II, *CsCNGC1.8* in cultivar I (10 days) and cultivar II, *CsCNGC1.9* in cultivar I, *CsCNGC10* in cultivar I (20 days), *CsCNGC17* in both cultivars, and *CsCNGC18* in cultivar I, *CsCNGC19* in cultivar I (10 days) and cultivar II, *CsCNGC2.1* in cultivar I (10 days), *CsCNGC2.4* in cultivar I (20 days), *CsCNGC2.6* in cultivar II, *CsCNGC4.1*, *CsCNGC4.2*, *CsCNGC4.3* and *CsCNGC4.4* in cultivar I (20 days), *CsCNGC7* in cultivar I (10 days) and *CsCNGC8* in cultivar I were those genes that have no change in expression after providing stress condition (Figure 8).

3.10 Expression validation of the citrus cyclic nucleotide-gated channel genes through quantitative reverse transcription-polymerase chain reaction

To explore the role and relationship between CNGC genes and drought stress, the citrus plant was treated with drought stress under different conditions (Figure 9). The results showed the expression level of different genes under no treatment and drought treatment at 10 and 20 days. According to the qRT-PCR results, the *CsCNGC1.4* gene had higher expression after 10 and 20 days of drought treatment compared to the expression level when no stress was applied (Figure 9). The same pattern of gene expression was observed for other members including *CsCNGC2.1*, *CsCNGC2.3*, *CsCNGC2.4*, *CsCNGC4.2*, *CsCNGC4.3*, *CsCNGC4.4* and *CsCNGC5*. The level of gene expression increased after 10 days of treatment and further increased after 20 days of treatment. *CsCNGC4.6* had different expression patterns, where the level of gene expression under controlled conditions was higher. Drought treatment for 10 days decreased the level of gene expression, while the level of gene expression was again increased after 20 days of drought stress but still lesser than the controlled condition. Two unique genes *CsCNGC13* and *PtCNGC14* had the same expression pattern being lesser expression under controlled conditions while increased after treatment with drought stress. Results suggest that these members of the CNGC gene family were sensitive to stress conditions, and thus are involved in stress regulation.

3.11 3D Structure prediction of CNGCs in citrus spp.

The protein structures that were predicted are having almost similar structures except for *CsCNGC1.4* and *PtCNGC14* which had unique structures (Figure 10). Three-dimensional structures of solely thirteen CNGC proteins were predicted because these were differentially expressed proteins. Predicted structures of all CNGC proteins were visualized in the interactive 1 preset of Pymol (Yuan et al., 2017) where different colors are used to represent alpha helices and beta sheets. Each CNGC protein contained alpha helices and beta sheets. The long spirals were representing alpha helices while wide arrows were representing beta sheets. The templates used by tR Rosetta for modeling the structure of *CsCNGC1.4* were 5VA1, 7NP4, 5U6O, and 6UQF. *CsCNGC1.4* had 55 alpha helices, *CsCNGC2.3* had 38 alpha helices, *CsCNGC2.4* had 37 alpha helices, and *CsCNGC4.3* had 18 alpha helices, *CsCNGC4.6* had 41 alpha helices, *PtCNGC14* had 24 alpha helices and *PtCNGC13* had 28 alpha helices. While *CsCNGC2.1* and *CsCNGC4.4* contained 27 alpha helices, *CsCNGC13* and *AbuCNGC13* contained 26 alpha helices. *CsCNGC1.4* had 14 beta sheets, *PtCNGC14* had 2 beta sheets, *CsCNGC2.1*, *CsCNGC13*, and *AbuCNGC13* contained 8 beta sheets while the rest contained 10 beta sheets. The predicted structures of all these CNGC proteins were almost similar except for *CsCNGC1.4* and *PtCNGC14* suggesting that these proteins are potentially functionally similar too.

4 Discussion

The CNGC family is characterized by the presence of a CNBD domain and 6 TM domains along with a pore region (Saand et al., 2015). In the present study, the CNGC gene family is reported in *C. sinensis*, *C. reticulata*, *C. grandis*, *A. buxfolia*, and *P. trifoliata*. The presence of Ion trans and CNBD domain in *C. sinensis*, *C. reticulata*, *C. grandis*, *A. buxfolia*, and *P. trifoliata* confirm the genes identified are true CNGC genes. Most of the proteins in *B. oleracea* (Kakar et al., 2017), *O. sativa* (Nawaz et al., 2014), *Z. mays* (Hao and Qiao, 2018), *T. aestivum* (Guo et al., 2018), *Z. jujuba mill* (Wang et al., 2020) were basic, unstable, hydrophilic, and localized to the plasma membrane and similar results were found for citrus spp. in the present study. The localization of citrus CNGC proteins to the plasma membrane means that these are ion channel proteins and are involved in the uptake of calcium across the membrane. Pangenome-wide analysis provides a comprehensive overview of diversity at the genomic level involving multiple species, which may lead to the identification of unique genes which are present in specific species instead of being present in all genomes under study (Tahir ul Qamar et al., 2020). Similarly, in this study two unique genes were identified including *CNGC13* and *CNGC14*. The

function of these members has not been yet identified in *A. thaliana*. Although, the function of these two members has been identified in *O. sativa* (Xu et al., 2017; Cui et al., 2020). The number of members in *C. grandis* and *P. trifoliata* is the same as the number of members in *B. rapa* while the number of members in Citrus *Spp.* is higher than that in *Z. mays* (12) (Hao and Qiao, 2018), *Z. jujuba* (15) (Wang et al., 2020), *O. sativa* (16) (Nawaz et al., 2014), *S. lycopersicum* (18) (Saand et al., 2015), *A. thaliana* (20) (Mäser et al., 2001), *P. bretschneideri* (21) (Chen et al., 2015), *B. oleracea* (26) (Kakar et al., 2017), and lower than that in *N. tobacum* (35) (Nawaz et al., 2018), *T. aestivum* (47) (Guo et al., 2018). The phylogenetic analysis classified the CNGC family members into four major groups and two sub-groups, I, II, III, IV-A, and IV-B that were the same as *A. thaliana* but some members were missing in Citrus *Spp.* The members that belong to the same group could have similar structures and functions. Group members in *C. sinensis*, *C. reticulata*, *C. grandis*, *A. buxfolia*, and *P. trifoliata* were named by the phylogenetic relationships with CNGC members of *A. thaliana*. However, CNGC1.1-1.5 and CNGC10 were present in group I of Citrus *Spp.* While CNGC13 which belongs to the same group was present only in *C. sinensis*, *A. buxfolia*, and *P. trifoliata*. CNGC5, CNGC7, and CNGC8 were present in group II of Citrus *Spp.* CNGC15.1-15.2, CNGC17, and CNGC18 were present in group III of Citrus *Spp.* While CNGC14 belongs to the same group and was only present in *P. trifoliata*, CNGC15.3 also belongs to the same group and was present in *C. reticulata*, *C. grandis*, *A. buxfolia*, and *P. trifoliata* except for *C. sinensis*. CNGC16 also belongs to the same group and was present in *C. sinensis*, *C. reticulata*, *C. grandis*, and *P. trifoliata* while CNGC16.1 and CNGC16.2 were present in *A. buxfolia*. CNGC19 was present in group IV-A of Citrus *Spp.*, while CNGC2.1-2.3 and CNGC4.1-4.6 were present in Group IV-B of Citrus *Spp.* CNGC2.4, CNGC2.5, and CNGC2.6 also belong to the same group where CNGC2.4 was present in *C. sinensis*, *C. reticulata*, *C. grandis*, and *P. trifoliata* except *A. buxfolia*, CNGC2.5 and CNGC2.6 were present in *C. sinensis*, *C. grandis* and *P. trifoliata* except *C. reticulata* and *A. buxfolia*. In the current study Group IV constituted the largest clade with 84 members while the clade of group II was the smallest with 29 members. While, in *A. thaliana* (Mäser et al., 2001) clade of group I was the largest and the clade of group IV was the smallest. In *B. rapa* (Li et al., 2019) group I constituted largest clade and clade of group IV-B was smallest. In *Z. mays* (Hao and Qiao, 2018) clade of group IV-B was largest and clade of group I was smallest. In *B. oleracea* (Kakar et al., 2017) clade of group IV was largest and clade of group II was smallest. In *P. bretschneideri* (Chen et al., 2015) clade of group I was largest and clade of group II and IV-A was smallest. In *O. sativa* clade of group III was largest and group II was smallest.

Results of chromosomal mapping suggested that most of the genes were present on chromosome 9 in *C. sinensis*, *C. reticulata*, *C. grandis*, *A. buxfolia*, and on chromosome 1 in

P. trifoliata. Minimum genes were present in chromosomes 3, 6, and 8 in *C. sinensis*, chromosome 3 in *C. reticulata*, *C. grandis*, and *A. buxfolia* while chromosome 2 and chromosome 8 in *P. trifoliata*. The distribution of CNGC genes on chromosomes in Citrus *Spp.* was different as compared to other plants in which the gene family is already reported including *B. oleracea* (Kakar et al., 2017) in which maximum genes were present on chromosome 1 and 5 and minimum genes were present on chromosome 7. *B. rapa* (Li et al., 2019) in which maximum genes were present on chromosome 1 and minimum genes were present on chromosomes 6, 7, and 9, *P. bretschneideri* (Chen et al., 2015) in which maximum genes were present on chromosomes 1, 8, and 15, and minimum genes were present at 2, 9, 13, 16 and 17, *N. tabacum* (Saand et al., 2015) in which chromosome 1 and 8 carried maximum genes and minimum genes were present at chromosome 22 and 11. The gene structures of *C. sinensis*, *C. reticulata*, *C. grandis*, *A. buxfolia*, and *P. trifoliata* were somewhat similar to *A. thaliana* as the number of exons and introns of Citrus plants that are being studied were not exactly same as *A. thaliana*, *O. sativa*, and other plants. Conserved motif analysis suggested that motifs for IQ domain, CaM binding motif, and CNB motifs were present in *C. sinensis*, *C. reticulata*, *C. grandis*, *A. buxfolia*, *P. trifoliata* as reported in *B. oleracea* (Kakar et al., 2017) in which all the above-mentioned motifs were present. *Z. jujube* (Wang et al., 2020) also had a similar pattern of motifs. Others include *N. tabacum* (Nawaz et al., 2018) in which CNB motif CaM binding motif and motif for IQ domain were present, and *T. aestivum* (Guo et al., 2018) in which Cyclic nucleotide binding motif and motif for IQ domain were present. In *Z. mays* (Hao and Qiao, 2018) motif 3 was the combination of both CaMB and motif for the IQ domain, while motif 4 was the CNB domain and motifs 1, 2, 5, 8, 9, and 10 were transmembrane domains. The motifs were closely related to CNGC motifs in *Z. mays*. Cis-regulatory elements (CREs) that were present in promoter regions of Citrus *Spp.* were mainly of four types light responsive, stress-related, hormone-related, and development related. In *Z. mays* (Hao and Qiao, 2018) hormones, stress, and development-related cis-regulatory elements were present. *O. sativa* (Nawaz et al., 2014), *Z. jujuba* (Wang et al., 2020), and *N. tabacum* (Nawaz et al., 2018) also contained all these stress-responsive elements. Cis-regulatory element analysis shows that the CNGC gene family is involved in plant response to light, hormone, and abiotic Gene duplication mainly contributes to the expansion of a gene family in plant species. In *P. bretschneideri* mainly segmental duplication has played role in the expansion of the CNGC gene family (Chen et al., 2015). In *Arabidopsis* CNGCs both segmental and tandem duplications contributed to the expansion of the CNGC gene family. Similarly, both segmental and tandem duplications played a role in the expansion of the CNGC gene family in *C. sinensis*, *C. reticulata*, *C. grandis*, *A. buxfolia*, and *P. trifoliata*. In *O. sativa* (Nawaz et al., 2014) three gene pairs were found to be segmentally duplicated including *OsCNGC1*/

OsCNGC2, *OsCNGC10/OsCNGC11*, *OsCNGC15/OsCNGC16*, and one gene pair was found to be tandemly duplicated including *OsCNGC2/OsCNGC3*. Hence, both tandem and segmental duplications contributed to the expansion of the CNGC gene family in *O. sativa* (Nawaz et al., 2014). In *N. tobacum* the CNGC gene family was also considered to be expanded through both segmental and tandem duplications (Nawaz et al., 2018). Most of the *OsCNGCs* were upregulated under abscisic acid treatment (ABA) i.e., 12 and indole acetic acid (IAA) treatment i.e., 11, and very few genes were upregulated under kinetin (KN) i.e., 2 and ethylene (ETH) treatment i.e., 6, where genes belonging to same groups showed similar expression patterns. Under cold stress *OsCNGCs* that were present in phylogenetic groups I, II, and III were upregulated and those present in group IV were downregulated where *OsCNGC6* exhibited the highest expression and *OsCNGC16* exhibited the lowest expression. Under pathogen stress where two phytopathogens were inoculated with 4 weeks old rice seedlings including *Pseudomonas fuscovaginae* and *Xanthomonas oryzae* pv. *oryzae* (*Xoo*) the expression patterns of *OsCNGCs* demonstrated that except *OsCNGC5* and *OsCNGC6* all other *OsCNGCs* were up-regulated under *Xoo* while all the fourteen *OsCNGCs* were significantly up-regulated under *P. fuscovaginae* inoculation. Thus, all the *OsCNGCs* that were duplicated were exhibiting similar expression patterns alongside relevance in their functions. *OsCNGC1* and *OsCNGC2* were duplicated genes and were also exhibiting similar expression patterns under abiotic stress i.e., Abscisic acid (ABA) and indole acetic acid (IAA) treatment and pathogenic stress that demonstrates that their functions were overlapping (Nawaz et al., 2014). The 10 duplicated gene pairs in *C. sinensis* exhibit similar expression patterns except *CsCNGC2.1/CsCNGC2.2* where *CsCNGC2.1* was highly up-regulated in cultivar I at 20 days drought stress and slightly down-regulated in cultivar II while that as not true for *CsCNGC2.2*. Among 10 duplicated gene pairs *CsCNGC1.8* was slightly up-regulated in cultivar I at 20 days drought stress, *CsCNGC1.9* was slightly down-regulated in cultivar II, *CsCNGC2.3*, *CsCNGC2.4* and *CsCNGC2.5* were slightly down-regulated in cultivar II, *CsCNGC2.4* was slightly up-regulated in cultivar I at 10 days drought stress, *CsCNGC2.6* was slightly down-regulated in cultivar I at 20 days drought stress while *CsCNGC7* and *CsCNGC8* in both cultivars and aforementioned genes in remaining cultivars were having no change in expression. Thus, we can hypothesize that duplicated genes exhibit similar expression patterns and function overlapping in Citrus *Spp.* too. It seems that some evolutionary events such as duplication could affect the members of CNGC gene family. On the other hand, mutations in the structure, including upstream/downstream site and coding sequence site of members could change the expression levels of CNGC genes (Abdullah et al., 2021; Faraji et al., 2021; Heidari et al., 2021). In *T. aestivum* (Guo et al., 2018),

O. sativa (Nawaz et al., 2014), *A. thaliana* (Mäser et al., 2001), *P. bretschneideri* (Chen et al., 2015), *Z. mays* (Hao and Qiao, 2018), *Z. jujuba* (Wang et al., 2020), and *S. lycopersicum* (Saand et al., 2015) the CNGC family members were different indicating that gene duplications and gene losses have played an important role in the creation of new genes and functions. The increase in the number of CNGC gene family members was an important event that contributed to the ability of these plants to adapt to changing environmental conditions.

The miRNAs are non-coding RNAs that regulate gene expression. In this study, a total of 226 putative miRNAs were identified that targeted 32 *CsCNGCs*. Several miRNAs were targeting each gene except *CsCNGC17* which was targeted by a single miRNA and *CsCNGC7* was targeted by 16 miRNAs. In *B. oleracea* 14 miRNAs were identified that targeted 17 *BoCNGCs* (Kakar et al., 2017). After eliminating false positives based on a threshold value of 5 there remained 5 miRNAs that targeted 9 *BoCNGCs*. Out of these miRNAs, bol-miR838days had five target genes while the rest of them were targeting only one gene. The majority of the miRNAs were related to cleavage while only two miRNAs were involved in the inhibition of translation of target genes. In *N. tobacum* 162 tobacco miRNAs were identified that targeted 18 *NtabCNGCs* (Nawaz et al., 2018). After eliminating false positives based on a threshold value of 4 there remained 79 miRNAs. While, after applying a threshold value of 3 there remained 6 miRNAs from 3 families that comprised 8 *NtabCNGCs*. Most of the genes were having target sites for multiple miRNAs except *NtabCNGC19* which contained the target site of a single miRNA. Prior studies support the evidence that miRNAs are involved in stress response and adaptation including topping and wounding in *N. tobacum* and miRNAs are also involved in drought signaling in rice (Root, 2016). The study done by (AAB et al., 2019) demonstrates a list of drought-tolerant plant crops with the involvement of genes of specific gene families and the role of their respective miRNAs. Hence, we can conclude that miRNAs in *CsCNGCs* will also be involved in their response to drought stress. PPI network analysis showed the interaction among citrus CNGC proteins as well as with the other citrus proteins. Higher connectivity was shown by CNGC and other genes which shows their involvement in pathways. The PPI results performed on BoCNGC proteins show that these proteins also have higher connectivity among themselves and with other proteins suggesting their integrated role in biotic, abiotic stress, and hyper-sensitivity resistance (Kakar et al., 2017). In maize, the PPI network analysis was conducted based on interactions found on STRING. Similarly, the *ZmCNGC* proteins also showed connectivity within the CNGC members as well as with the homologous proteins from *Arabidopsis* (Hao and Qiao, 2018). In cotton, the functional interaction analysis demonstrated that most of the *GhCNGC* proteins were found to have higher connectivity with a receptor kinase present in the plasma membrane, FLS2 that activates immune signaling. Several

other proteins were showing interactions with RSTK, MOL, and TAD3 which are involved in growth and developmental functions (Zhao et al., 2022). These results regarding interactions of CNGC family members show their contribution of these genes to the functional as well as regulatory diversity in plants and might be helpful in future research to better understand the functions of CNGC genes. As CNGCs are ion channels, so according to GO enrichment these genes are present in the plasma membrane, act as transmembrane ion transporters, and are involved in ion channel activity, potassium and calcium ion transport activity, and protein binding activity. In *Brassica oleracea*, according to biological processes, the BoCNGCs are associated with ion channel activity for transmembrane transport, negative regulation of defense responses, salicylic acid biosynthesis, responses to chitin, and plant-type hypersensitive responses. BoCNGCs are present in the plasma membrane and participate in cellular activities related to transduction, binding, and transport (Kakar et al., 2017).

Expression patterns of CsCNGC in leaves samples under drought stress at 10 and 20 days indicated that three genes namely *CsCNGC1.4*, *CsCNGC2.1*, and *CsCNGC4.2* were highly up-regulated while *CsCNGC4.6* was highly down-regulated. Out of two unique genes identified in this study, one is present in *C. sinensis*, *CsCNGC13*. The expression analysis of this gene in two cultivars is down-regulated under drought stress which shows some specialty in terms of abiotic stress regulation. These results were similar to the ones demonstrated by earlier studies such as expression patterns of *N. tabacum* showed that 18 CNGC genes (*NtabCNGC2*, 3, 5–7, 14, 16–21, and 29–34) were up-regulated under Calmodulin stress, 16 CNGC genes (*NtabCNGC1*, 3–7, 14, 16, 17, 26–28, and 30–33) under drought stress and 10 CNGC genes (*NtabCNGC2*, 3, 5–7, 14, 16, 17, 19 and 20) under cold stress and some genes were downregulated in response to these stresses (Nawaz et al., 2018). Expression patterns of *O. sativa* demonstrated that 10 OsCNGC genes were up-regulated under cold stress, and group IV members were down-regulated under cold stress (Nawaz et al., 2014). In *Z. jujuba* *ZjCNGC10*, 8, 2, and 15 were downregulated under cold stress (24 h), and *ZjCNGC4* and 12 were up-regulated under cold stress (1 h). The majority of *ZjCNGCs* were down-regulated after being treated with salt stress, particularly group III members, and the same was the case for *ZjCNGCs* under alkaline stress (Wang et al., 2020). In *B. oleracea* 13 BoCNGCs genes were up-regulated under cold stress. However, more BoCNGCs were up-regulated under pathogen stress of *Xanthomonas campestris* pv. *campestris* (Xcc) as compared to those treated with cold stress (Kakar et al., 2017). Promoter and expression analysis revealed some genes that have variable expression under abiotic stress. It is hypothesized that several hormones and abiotic stress-related elements control the variable expression level of CsCNGCs under various abiotic stress conditions. As a result, this study confers

that these genes can be used in future research due to their importance in abiotic stress response.

5 Conclusion

In this study, a total of 32 genes in *C. sinensis*, 27 genes in *C. reticulata*, 30 genes in *C. grandis*, 31 genes in *A. buxfolia*, and 30 in *P. trifoliata* were identified as belonging to the CNGCs gene family. CNGC genes were identified based on CNGC-specific motifs and domains. *CsCNGCs*, *CreCNGCs*, *CgCNGCs*, *AbuCNGCs*, and *PtCNGCs* have diversity in their functions, protein lengths, and gene structures. Previously, Genome-wide studies have been done on the CNGC gene family in other plants but the present study is illustrating a pangenome-wide representation of the CNGC gene family among five Citrus spp. To the best of our knowledge, this is the first research implementing the concept of pangenome-wide analysis and will be helpful for further pan-genome wide studies on other plants in the future. This analysis provided a detailed explanation regarding the pattern of evolution of CNGCs in Citrus spp. their intron-exon patterns, distribution of CNGC genes on chromosomes, prediction of CNGC specific motifs and domains, duplication type, along with promoter region analysis indicating which regulatory elements are more likely to influence the expression of particular genes. Phylogenetic analysis revealed that CNGCs of these five citrus species were clustered into four major groups and two sub-groups. A few CNGCs in the groups were missing or might be duplicated during evolution. CREs analysis reveals the association of gene families in response to abiotic stresses. The miRNAs also play a role in the response of CNGC genes to drought stress alongside regulating the expression of these genes. PPI network analysis also provided insights into their connectivity suggesting their involvement in functional regulation. GO enrichment was executed to understand the functions of CNGCs at the molecular level. Expression profiling was done on tissue-specific data of *C. sinensis* under drought stress that demonstrates that *CsCNGC1.4*, *CsCNGC2.1*, *CsCNGC4.2* were highly upregulated and *CsCNGC4.6* was highly downregulated under drought stress. Unique genes *CsCNGC13* and *PtCNGC14* also showed higher expression in drought stress. These genes can be used in further studies to develop stress-resistant crops. One can visualize and understand the genomic diversity among the Citrus species being examined. We have observed significant inter and intra-species diversity of the CNGC gene family members. The diversity observed could be due to differences in sequencing approaches. Therefore, further experiments are required to get deep insights.

Data availability statement

The original contributions presented in the study are included in the article/[Supplementary Material](#), further inquiries can be directed to the corresponding author.

Author contributions

KZ and MR drafted the manuscript, prepared illustrations, and discussed the content with the MS and KF. MT conceived this research topic and revised the contents of the manuscript. FA revised the manuscript. AA and MA were involved in the final development of the manuscript and funding acquisition. All authors contributed to the article and approved the submitted version.

Funding

The authors are thankful to the Researchers Supporting Project number (RSP 2022R491), King Saud University, Riyadh, Saudi Arabia.

References

- Aab, K. U. K., Nawaz, Z., and Ahmed, J. (2019). Recent trend of genome-wide multigene family analysis and their role in plant drought tolerance. *Ann. Agric. Crop Sci.* 4, 1046.
- Abdullah, Faraji, S., Mehmood, F., Malik, H. M. T., Ahmed, I., Heidari, P., et al. (2021). The GASA gene family in *Theobroma cacao*: Genome wide identification and expression analyses. *Agronomy* 11, 1425. doi:10.3390/agronomy11071425
- Bailey, T. L., Boden, M., Buske, F. A., Frith, M., Grant, C. E., Clementi, L., et al. (2009). MEME Suite: Tools for motif discovery and searching. *Nucleic Acids Res.* 37, 202–208. doi:10.1093/nar/gkp335
- Bender, K. W., and Snedden, W. A. (2013). Calmodulin-related proteins step out from the shadow of their namesake. *Plant Physiol.* 163, 486–495. doi:10.1104/pp.113.221069
- Bhusal, R. C., Mizutani, F., and Laban Rutt, K. (2002). Selection of rootstocks for flooding and drought tolerance in citrus species. *Pak. J. Biol. Sci.* 5, 509–512. doi:10.3923/pjbs.2002.509.512
- Chen, C., Chen, H., Zhang, Y., Thomas, H. R., Frank, M. H., He, Y., et al. (2020). TBtools: An integrative toolkit developed for interactive analyses of big biological data. *Mol. Plant* 13, 1194–1202. doi:10.1016/j.molp.2020.06.009
- Chen, J., Yin, H., Gu, J., Li, L., Liu, Z., Jiang, X., et al. (2015). Genomic characterization, phylogenetic comparison and differential expression of the cyclic nucleotide-gated channels gene family in pear (*Pyrus bretschneideri* Rehd.). *Genomics* 105, 39–52. doi:10.1016/j.ygeno.2014.11.006
- Cheng, S. H., Willmann, M. R., Chen, H. C., and Sheen, J. (2002). Calcium signaling through protein kinases. The Arabidopsis calcium-dependent protein kinase gene family. *Plant Physiol.* 129, 469–485. doi:10.1104/pp.005645
- Cui, Y., Lu, S., Li, Z., Cheng, J., Hu, P., Zhu, T., et al. (2020). Cyclic nucleotide-gated ion channels 14 and 16 promote tolerance to heat and chilling in rice. *Plant Physiol.* 183, 1794–1808. doi:10.1104/pp.20.00591
- Dai, X., Zhuang, Z., and Zhao, P. X. (2018). PsRNA Target: A plant small RNA target analysis server (2017 release). *Nucleic Acids Res.* 46, W49–W54. doi:10.1093/nar/gky316
- Demidchik, V., Shabala, S., Isayenkova, S., Cuin, T. A., and Pottosin, I. (2018). Calcium transport across plant membranes: Mechanisms and functions. *New Phytol.* 220, 49–69. doi:10.1111/nph.15266
- Du, Z., Su, H., Wang, W., Ye, L., Wei, H., Peng, Z., et al. (2021). The trRosetta server for fast and accurate protein structure prediction. *Nat. Protoc.* 16, 5634–5651. doi:10.1038/s41596-021-00628-9
- Duszyn, M., Świeżawska, B., Szmidt-Jaworska, A., and Jaworski, K. (2019). Cyclic nucleotide gated channels (CNGCs) in plant signalling—current knowledge and perspectives. *J. Plant Physiol.* 241, 153035. doi:10.1016/j.jplph.2019.153035
- Faraji, S., Heidari, P., Amouei, H., Filiz, E., Abdullah, and Poczai, P. (2021). Investigation and computational analysis of the sulfotransferase (Sot) gene family in potato (*Solanum tuberosum*): Insights into sulfur adjustment for proper development and stimuli responses. *Plants* 10, 2597. doi:10.3390/plants10122597
- Gasteiger, E., Gattiker, A., Hoogland, C., Ivanyi, I., Appel, R. D., and Bairoch, A. (2003). ExPASy: The proteomics server for in-depth protein knowledge and analysis. *Nucleic Acids Res.* 31, 3784–3788. doi:10.1093/nar/gkg563
- Golicz, A. A., Batley, J., and Edwards, D. (2016). Towards plant pangenomics. *Plant Biotechnol. J.* 14, 1099–1105. doi:10.1111/pbi.12499
- Guo, J., Islam, A., Lin, H., Ji, C., Duan, Y., and Liu, P. (2018). Genome-wide identification of cyclic nucleotide-gated ion channel gene family in wheat and functional analyses of TaCNGC14 and TaCNGC16. *Front. Plant Sci.* 9, 1–17. doi:10.3389/fpls.2018.00018
- Hao, L., and Qiao, X. (2018). Genome-wide identification and analysis of the CNGC gene family in maize. *PeerJ* 6, e5816. doi:10.7717/peerj.5816
- He, Y., Liu, X., Ye, L., Pan, C., Chen, L., Zou, T., et al. (2016). Genome-wide identification and expression analysis of two-component system genes in tomato. *Int. J. Mol. Sci.* 17 (8), 1204. doi:10.3390/ijms17081204
- Heidari, P., AbdullaFaraji, S., and Poczai, P. (2021). Magnesium transporter gene family: Genome-wide identification and characterization in theobroma cacao, corchorus capsularis, and gossypium hirsutum of family malvaceae. *Agronomy* 11, 1651. doi:10.3390/agronomy11081651
- Hu, B., Jin, J., Guo, A. Y., Zhang, H., Luo, J., and Gao, G. (2015). Gsds 2.0: An upgraded gene feature visualization server. *Bioinformatics* 31, 1296–1297. doi:10.1093/bioinformatics/btu817
- Hu, Y., Zhang, T., Liu, Y., Li, Y., Wang, M., Zhu, B., et al. (2021). Pumpkin (*Cucurbita moschata*) HSP20 gene family identification and expression under heat stress. *Front. Genet.* 12, 753953–754015. doi:10.3389/fgene.2021.753953

Conflict of interest

The authors declare that the research was conducted in the absence of any commercial or financial relationships that could be construed as a potential conflict of interest.

Publisher's note

All claims expressed in this article are solely those of the authors and do not necessarily represent those of their affiliated organizations, or those of the publisher, the editors and the reviewers. Any product that may be evaluated in this article, or claim that may be made by its manufacturer, is not guaranteed or endorsed by the publisher.

Supplementary material

The Supplementary Material for this article can be found online at: <https://www.frontiersin.org/articles/10.3389/fgene.2022.1034921/full#supplementary-material>

- Ihaka, R., and Gentleman, R. (1996). R: A language for data analysis and graphics. *J. Comput. Graph. Stat.* 5, 299–314. doi:10.1080/10618600.1996.10474713
- Ismail, S., Alsowayeh, N., Abbasi, H. W., Albutti, A., and Tahir, M. (2022). Pan-genome-assisted computational design of a multi-epitopes-based vaccine candidate against Helicobacter cinaedi. *Int. J. Environ. Res. Public Health* 19 (18), 11579. doi:10.3390/ijerph191811579
- Jha, S. K., Sharma, M., and Pandey, G. K. (2016). Role of cyclic nucleotide gated channels in stress management in plants. *Curr. Genomics* 17:315–329. doi:10.2174/13892091766160331202125
- Juniper, J., Evans, R., Pritzel, A., Green, T., Figurnov, M., Ronneberger, O., et al. (2021). Highly accurate protein structure prediction with AlphaFold. *Nature* 596, 583–589. doi:10.1038/s41586-021-03819-2
- Kakar, K. U., Nawaz, Z., Kakar, K., Ali, E., Almoneafy, A. A., and Ullah, R. (2017). Comprehensive genomic analysis of the CNGC gene family in *Brassica oleracea*: Novel insights into synteny, structures, and transcript profiles. *BMC Genomic* 18, doi:10.1186/s12864-017-4244-y
- Köhler, C., and Neuhaus, G. (2000). Characterisation of calmodulin binding to cyclic nucleotide-gated ion channels from *Arabidopsis thaliana*. *FEBS Lett.* 471, 133–136. doi:10.1016/S0014-5793(00)01383-1
- Koshita, Y., and Takahara, T. (2004). Effect of water stress on flower-bud formation and plant hormone content of satsuma Mandarin (*Citrus unshiu* Marc.). *Sci. Hortic.* 99, 301–307. doi:10.1016/S0304-4238(03)00113-4
- Kudla, J., Becker, D., Grill, E., Hedrich, R., Hippler, M., Kummer, U., et al. (2018). Advances and current challenges in calcium signaling. *New Phytol.* 218, 414–431. doi:10.1111/nph.14966
- Lecourieux, D., Raneva, R., and Pugin, A. (2006). Calcium in plant defence-signalling pathways. *New Phytol.* 171, 249–269. doi:10.1111/j.1469-8137.2006.01777.x
- Lescot, M., Déhais, P., Thijss, G., Marchal, K., Moreau, Y., Van De Peer, Y., et al. (2002). PlantCARE, a database of plant cis-acting regulatory elements and a portal to tools for *in silico* analysis of promoter sequences. *Nucleic Acids Res.* 30, 325–327. doi:10.1093/nar/30.1.325
- Letunic, I., and Bork, P. (2021). Interactive tree of life (iTOL) v5: An online tool for phylogenetic tree display and annotation. *Nucleic Acids Res.* 49, W293–W296. doi:10.1093/nar/gkab301
- Li, Q., Yang, S., Ren, J., Ye, X., jiang, X., and Liu, Z. (2019). Genome-wide identification and functional analysis of the cyclic nucleotide-gated channel gene family in Chinese cabbage. *Biotech* 9, 114. doi:10.1007/s13205-019-1647-2
- Librado, P., and Rozas, J. (2009). DnaSP v5: A software for comprehensive analysis of DNA polymorphism data. *Bioinformatics* 25, 1451–1452. doi:10.1093/bioinformatics/btp187
- Liu, H., Wang, X., Liu, S., Huang, Y., Guo, Y.-X., Xie, W.-Z., et al. (2022). Citrus pan-genome to breeding database (CPBD): A comprehensive genome database for citrus breeding. *Mol. Plant.* doi:10.1016/J.MOLP.2022.08.006
- Liu, Y., Heying, E., and Tanumihardjo, S. A. (2012). History, global distribution, and nutritional importance of citrus fruits. *Compr. Rev. Food Sci. Food Saf.* 11, 530–545. doi:10.1111/j.1541-4337.2012.00201.x
- Liu, Y., Tahir Ul Qamar, M., Feng, J. W., Ding, Y., Wang, S., Wu, G., et al. (2019). Comparative analysis of miniature inverted-repeat transposable elements (MITEs) and long terminal repeat (LTR) retrotransposons in six Citrus species. *BMC Plant Biol.* 19, 140. doi:10.1186/s12870-019-1757-3
- Luan, S. (2009). The CBL-CIPK network in plant calcium signaling. *Trends Plant Sci.* 14, 37–42. doi:10.1016/j.tplants.2008.10.005
- Marchler-bauer, A., Lu, S., Anderson, J. B., Chitsaz, F., Derbyshire, M. K., Deweese-scott, C., et al. (2011). Cdd : A conserved domain database for the functional annotation of proteins. *Nucleic Acids Res.* 39, 225–229. doi:10.1093/nar/gkq1189
- Mäser, P., Thomine, S., Schroeder, J. I., Ward, J. M., Hirschi, K., Sze, H., et al. (2001). Phylogenetic relationships within cation transporter families of *Arabidopsis*. *Plant Physiol.* 126, 1646–1667. doi:10.1104/pp.126.4.1646
- Nawaz, Z., Kakar, K. U., Saand, M. A., and Shu, Q. Y. (2014). Cyclic nucleotide-gated ion channel gene family in rice: identification, characterization and experimental analysis of expression response to plant hormones, biotic and abiotic stresses. *BMC Genomics* 15, 853–918. doi:10.1186/1471-2164-15-853
- Nawaz, Z., Kakar, K. U., Ullah, R., Yu, S., Zhang, J., and Shu, Q. (2018). Genomics Genome-wide identification, evolution and expression analysis of cyclic nucleotide-gated channels in tobacco (*Nicotiana tabacum* L.) ⋆. *Genomics*, 1. doi:10.1016/j.ygeno.2018.01.010
- Nguyen, L. T., Schmidt, H. A., Von Haeseler, A., and Minh, B. Q. (2015). IQ-TREE: A fast and effective stochastic algorithm for estimating maximum-likelihood phylogenies. *Mol. Biol. Evol.* 32, 268–274. doi:10.1093/molbev/msu300
- Osakabe, Y., Yamaguchi-Shinozaki, K., Shinozaki, K., and Tran, L. S. P. (2014). ABA control of plant macroelement membrane transport systems in response to water deficit and high salinity. *New Phytol.* 202, 35–49. doi:10.1111/nph.12613
- Pingping, W. U., Chubin, W. U., and Biyan, Z. (2017). Drought stress induces flowering and enhances carbohydrate accumulation in averrhoa carambola. *Hortic. Plant J.* 3, 60–66. doi:10.1016/j.hpj.2017.07.008
- Potter, S. C., Eddy, S. R., Park, Y., Lopez, R., Finn, R. D., and Hmmer, T. (2018). HMMER web server : 2018 update. *Nucleic Acids Res.* 46, 200–204. doi:10.1093/nar/gky448
- Ranty, B., Aldon, D., Cotelle, V., Galaud, J., Thuleau, P., and Mazars, C. (2016). Calcium sensors as key hubs in plant responses to biotic and abiotic stresses. *Front. Plant Sci.* 7, 327–7. doi:10.3389/fpls.2016.00327
- Rhee, S. Y., Beavis, W., Berardini, T. Z., Chen, G., Dixon, D., Doyle, A., et al. (2003). The Arabidopsis information resource (TAIR): A model organism database providing a centralized, curated gateway to Arabidopsis biology, research materials and community. *Nucleic Acids Res.* 31, 224–228. doi:10.1093/nar/gkg076
- Root, R. (2016). MicroRNA signatures of drought signaling in rice root. *PLoS One* 11, e0156814. doi:10.1371/journal.pone.0156814
- Saand, M. A., Xu, Y. P., Li, W., Wang, J. P., and Cai, X. Z. (2015). Cyclic nucleotide gated channel gene family in tomato: Genome-wide identification and functional analyses in disease resistance. *Front. Plant Sci.* 6, 303. doi:10.3389/fpls.2015.00303
- Schultz, J., Copley, R. R., Doerks, T., Ponting, C. P., Bork, P., Road, S. P., et al. (2000). Smart : A web-based tool for the study of genetically mobile domains. *Nucleic Acids Res.* 28, 231–234. doi:10.1093/nar/28.1.231
- Shannon, P., Markiel, A., Ozier, O., Baliga, N. S., Wang, J. T., Ramage, D., et al. (1971). Cytoscape: A software environment for integrated models. *Genome Res.* 13, 426. doi:10.1101/gr.1239303.metabolite
- Tahir ul Qamar, M., Zhu, X., Khan, M. S., Xing, F., and Chen, L. L. (2020). Pan-genome: A promising resource for noncoding RNA discovery in plants. *Plant Genome* 13, e20046. doi:10.1002/tpg2.20046
- Tahir Ul Qamar, M., Zhu, X., Xing, F., and Chen, L.-L. (2019). ppsPCP: a plant presence/absence variants scanner and pan-genome construction pipeline. *Bioinformatics* 35, 4156–4158. doi:10.1093/bioinformatics/btz168
- Talke, I. N., Blaudez, D., Maathuis, F. J. M., and Sanders, D. (2003). CNGCs : Prime targets of plant cyclic nucleotide signalling. *Trends Plant Sci.* 8, 286–293. doi:10.1016/S1360-1385(03)00099-2
- Tettelin, H., Masiagnani, V., Cieslewicz, M. J., Donati, C., Medini, D., Ward, N. L., et al. (2005). Genome analysis of multiple pathogenic isolates of *Streptococcus agalactiae*: Implications for the microbial “pan-genome”. *Proc. Natl. Acad. Sci. U. S. A.* 102, 13950–13955. doi:10.1073/pnas.0506758102
- Trudeau, M. C., and Zagotta, W. N. (2002). Mechanism of calcium/calmodulin inhibition of rod cyclic nucleotide-gated channels. *Proc. Natl. Acad. Sci. U. S. A.* 99, 8424–8429. doi:10.1073/pnas.122015999
- Vaattovaara, A., Lepälä, J., Salojärvi, J., and Wrzaczek, M. (2019). High-throughput sequencing data and the impact of plant gene annotation quality. *J. Exp. Bot.* 70, 1069–1076. doi:10.1093/jxb/ery434
- Wang, J. P., Munyampundu, J. P., Xu, Y. P., and Cai, X. Z. (2015). Phylogeny of plant calcium and calmodulin-dependent protein kinases (CcaMKs) and functional analyses of tomato CCaMK in disease resistance. *Front. Plant Sci.* 6, 1075–1115. doi:10.3389/fpls.2015.01075
- Wang, L., Li, M., Liu, Z., Dai, L., Zhang, M., Wang, L., et al. (2020). Genome-wide identification of CNGC genes in Chinese jujube (*Ziziphus jujuba* Mill.) and *ZjCNGC2* mediated signalling cascades in response to cold stress. *BMC Genomics* 21, 191–216. doi:10.1186/s12864-020-6601-5
- Wang, X., Xu, Y., Zhang, S., Cao, L., Huang, Y., Cheng, J., et al. (2017). Genomic analyses of primitive, wild and cultivated citrus provide insights into asexual reproduction. *Nat. Genet.* 49, 765–772. doi:10.1038/ng.3839
- Xu, Y., Yang, J., Wang, Y., Wang, J., Yu, Y., Long, Y., et al. (2017). OsCNGC13 promotes seed-setting rate by facilitating pollen tube growth in stylar tissues. *PLoS Genet.* 13, e1006906–e1006925. doi:10.1371/journal.pgen.1006906
- Yang, T., and Poovaiah, B. W. (2003). Calcium/calmodulin-mediated signal network in plants. *Trends Plant Sci.* 8, 505–512. doi:10.1016/j.tpls.2003.09.004
- Yu, C. S., Chen, Y. C., Lu, C. H., and Hwang, J. K. (2006). Prediction of protein subcellular localization. *Proteins* 64, 643–651. doi:10.1002/prot.21018
- Yuan, S., Chan, H. C. S., and Hu, Z. (2017). Using PyMOL as a platform for computational drug design. *WIREs Comput. Mol. Sci.* 7, 1–10. doi:10.1002/wcms.1298
- Zanini, S. F., Bayer, P. E., Wells, R., Snowdon, R. J., Batley, J., Varshney, R. K., et al. (2022). Pangenomics in crop improvement—From coding structural variations to finding regulatory variants with pangenome graphs. *Plant Genome* 15, 20177–e20218. doi:10.1002/tpg2.20177
- Zhao, J., Peng, S., Cui, H., Li, P., Li, T., Liu, L., et al. (2022). Dynamic expression, differential regulation and functional diversity of the CNGC family genes in cotton. *Int. J. Mol. Sci.* 23, 2041. doi:10.3390/ijms23042041